Design and Simulation of Fabry-Perot Antennas

Major Project Report

Submitted in fulfillment of the requirements
for the degree of

Master of Technology
in
Electronics & Communication Engineering
(Communication Engineering)

By

Honey Dhandhukia
(18MECC07)

Electronics & Communication Engineering Department
Institute of Technology
Nirma University
Ahmedabad-382 481

Design and Simulation of Fabry-Perot Antennas

Major Project Report

Submitted in fulfillment of the requirements
for the degree of

Master of Technology
in
Electronics & Communication Engineering
(Communication Engineering)

By

Honey Dhandhukia
(18MECC07)

Under the guidance of

Internal Project Guide:
Dr. Dhaval Pujara
Professor, Electronics & Communication Department,
Institute of Technology,
Nirma University, Ahmedabad.

Electronics & Communication Engineering Department
Institute of Technology
Nirma University
Ahmedabad-382 481

Declaration

This is to certify that the thesis comprises my original work towards the degree of Master of Technology in Communication Engineering at Nirma University and has not been submitted elsewhere for a degree. Due acknowledgment has been made in the text to all other material used.

-Honey Dhandhukia

(18MECC07)

NIRMA UNIVERSITY
INSTITUTE OF TECHNOLOGY
NAAC ACCREDITED 'A' GRADE

Certificate

This is to certify that the Major Project entitled "**Design and Simulation of Fabry-Perot Antennas**" submitted by **Honey Dhandhukia (18MECC07)**, towards the fulfilment of the requirements for the degree of Master of Technology in Electronics & Communication (Communication Engineering), Nirma University, Ahmedabad, is the record of work carried out by her under our supervision and guidance. In our opinion, the submitted work has reached a level required for being accepted for examination. The results embodied in this major project, to the best of my knowledge, haven't been submitted to any other university or institution for the award of any degree or diploma.

Date: Place: Ahmedabad

Dr. Dhaval Pujara
Internal Guide,
Professor EC Department,
Institute of Technology,
Nirma University, Ahmedabad.

Dr. Yogesh Trivedi
Program Coordinator,
Professor EC Department,
Institute of Technology,
Nirma University, Ahmedabad.

Dr. Dhaval Pujara
Professor and Head of EC Department,
Institute of Technology,
Nirma University, Ahmedabad.

Dr. Rajesh Patel
Director,
Institute of Technology,
Nirma University, Ahmedabad.

ACKNOWLEDGEMENT

It is indeed a pleasure to acknowledge and express my sincere gratitude to those who have always supported me throughout my project work.

I take this opportunity to express my sincere gratitude to my guide Dr. Dhaval Pujara for pointing the need and scope of work and continuous encouragement during the project work. It is my privilege to have carried out this project work under his guidance. I am highly obliged as he has devoted his valuable time and expertise knowledge.

I extend my sincere thanks to Mr. Jay Gupta for his suggestions and illuminating discussions at various stages of my project. I extend my thanks to Nirma university for providing excellent infrastructure. And my heartfelt appreciation to my friends and colleagues who have rendered their support for the completion of the project.

I am grateful to my brother and fiancé for their moral support and loving care. Whatever I have achieved in my life is due to the continuous guidance, motivation and blessings of my parents. I dedicate my thesis work to my parents.

-Honey Dhandhukia

(18MECC07)

LIST OF FIGURES

LIST OF TABLES

ABBREVIATION USED

EBG	Electromagnetic Band-Gap
EM	Electromagnetic
FPA	Fabry-Perot Antenna
FPCA	Fabry-Perot Cavity Antenna
FPI	Fabry-Perot Interferometer
FPRA	Fabry-Perot Resonator Antenna
FSS	Frequency Selective Surface
GBA	Gaussian Beam Antenna
HFSS	High Frequency Structure Simulator
LWA	Leaky Wave Antenna
MBA	Multiple Beam Antenna
PEC	Perfect Electric Conductor
PRS	Partially Reflecting Surface
RF	Radio Frequency

ABSTRACT

Horn antennas are widely used in the areas of satellite tracking, communication dishes, radio astronomy, as feeds for reflectors and lenses, as common elements in phased arrays, as a standard for calibration and gain measurements in laboratories for other high gain antennas, as a medium-gain antenna, and as feed clusters for Multiple Beam Antennas (MBAs). The basic requirements of these antennas are high directivity and gain, low return loss, low sidelobe level, low cross-polarization, and a purely metallic structure. In many practical applications, increasing the gain of a horn antenna becomes one of the major requirements. The gain of the horn antenna can be increased by several methods. Two of the conventional methods are: (i) by increasing the aperture size of the horn antenna and (ii) by forming an array of horn antennas to increase the overall gain. However, these methods suffer from a few limitations including the bulkier and complex antenna structure. One of the fascinating techniques to improve the gain of a horn antenna is to place a partially reflecting surface in front of an antenna at a particular distance. In the open literature, such a concept is described as Fabry-Perot Antenna (FPA). The present work is focused on the gain enhancement of horn antenna using a Fabry-Perot cavity approach.

A Fabry-Perot Antenna (FPA) primarily consists of a radiator, a partially reflecting surface (PRS), and a ground plane. It possesses the capability of increasing the aperture efficiency of an antenna. This thesis represents a complete procedure to be followed for designing a Fabry-Perot horn antenna for various configurations like a circular waveguide, pyramidal horn, conical horn, and cluster of conical horn antennas. It includes a complete theoretical explanation for various types of material used for PRS and the performance parameters of antenna-like return loss, directivity, gain, and radiation pattern are discussed. Exhaustive parametric analysis is carried out for all the proposed antennas. There is a significant improvement in gain and directivity performance for the proposed Fabry-Perot horn antenna. For pyramidal horn and conical horn with PRS improvement of 2.21 dBi and 2.02 dBi are accounted respectively. Increment of 6.58 dB in the directivity of conical horn antenna was observed and improvement in radiation pattern is observed for conical horn and cluster of the conical horn antenna. Analytical calculations and the simulations are performed by using electromagnetic solver HFSSv2014.

CHAPTER-1

INTRODUCTION

1.1 BACKGROUND

Antennas are metallic structures used to transmit and receive electromagnetic energy. It converts the RF signal traveling inside the conductor into an electromagnetic wave. Antennas are classified based on types of structure, for example, wire antennas, reflector antennas, aperture antennas, microstrip antennas, array antennas, and lens antennas. Among all the types of antenna, aperture antennas are the most widely used antenna.

Aperture antenna consists of an opening through which electromagnetic waves are transmitted and received. There are four types of aperture antennas: open-ended waveguides, horn antennas, reflector antennas, and lens antennas. Aperture antennas have advantages compared to wire antennas such as they are medium to the high gain antenna due to larger effective area, more directional radiation pattern, and high-power handling capacity.

Horn antenna is an open-ended waveguide with flaring and is extensively used due to its highly directional property. Sir Jagdish Chandra Bose was the first scientist who successfully constructed a horn antenna in the early 1800s. Horn antenna finds a wide range of applications such as a source antenna for radiation pattern measurements in the laboratory, as standard gain horns to evaluate the gain of antennas used for satellite communications, remote sensing, radar, etc. They are extensively used as primary and secondary feed to reflector antenna for various space applications such as global coverage; Telemetry, Tracking, and Control (TT&C); and as feed clusters for Multiple Beam Antennas (MBAs).

The basic requirements of horn antenna used for satellite communication are high directivity and gain, low return loss, low sidelobe level, purely metallic structure. The traditional way to achieve high directivity and gain in an antenna is by increasing the aperture size to produce a highly directional radiation pattern or to form an antenna array. However, these methods make the feeding mechanism and antenna system bulkier and more complex. To overcome this problem G. V. Trentini in the year 1956 proposed the concept of multiple reflections of electromagnetic waves between two planes to increase the directivity and gain of a waveguide antenna [1]. It was in the year 2001 when this concept found the similarity with Fabry-Perot Interferometer (FPI) widely used in optics and the name arose as Fabry-Perot Antennas (FPA).

Thereafter many authors used the principle of Fabry-Perot Interferometer (FPI) to enhance the directivity and gain of the antenna with titles like Electromagnetic Bandgap antennas (EBG), Fabry-Perot Cavity Antenna (FPCA), Fabry-Perot Resonator Antenna (FPRA), Leaky Wave Antennas (LWAs), and Fabry-Perot Antennas (FPAs). They provide highly directional properties allowing gain to be increased when compared to the conventional single feed system, which increased their deployment in wireless communication systems and radar applications. Several papers have been published and a few of them are discussed in section 1.3.

1.2 PROBLEM STATEMENT

Horn antennas used for applications such as wireless communication, radar sensing, satellite communication, point to point communications, etc., have a very specific requirements such as high directivity and gain, low return loss, low sidelobe levels, and low cross-polarization. In addition to these requirements, one boundary been drawn of the size of the horn so that it does not increase the weight of payloads when it is installed for space communication in the satellite. Thus, with the restriction over the size and weight, it is very challenging for an antenna designer to develop a high gain antenna working over a specific frequency range.

Thus, the prime objective of the thesis is designing and simulating a horn antenna with increased gain using the concept of the Fabry-Perot cavity. The problem statement is as follow:

To improve the gain of a horn antenna by using the Fabry-Perot cavity concept.

1.3 LITERATURE SURVEY

Since the introduction of the concept of Fabry-Perot resonator, in the year 1956, many research papers have been published in diversified areas related to antenna design. Some of the classical papers are highlighted in the subsequent paragraphs.

G.V. Trentini [1] has investigated the mathematical interpretation of multiple reflections between two parallel planes. He has used this concept in the antenna by placing the partially reflecting surface in front of a waveguide. Different types of partially reflecting surfaces, for example, movable wire grid, dielectric plate glass, capacitive and inductive strip grating, and perforated sheets are being investigated and their effects on the performance of the antenna are being discussed. The paper concludes that the adjustment of the distance between two sheets is very critical and they must be perfectly plane and parallel to each other. There is an improvement in the performance of antenna with directivity, gain, and radiation pattern.

A. P. Feresidis, et. al [2] investigated a high gain planar antenna using an optimized partially reflecting surface (PRS) placed in front of a waveguide aperture. It states that the way to increase gain and bandwidth of resonant structure is to optimize the reflection characteristics of PRS, which is characterized by its reflection coefficient. Authors have used a ray theory to investigate the reflection coefficient of different PRSs. For a conducting array of elements, the magnitude of the reflection coefficient decreases with an increase in frequency. They have carried out a parametric analysis on several geometries

such as dipoles, crossed dipoles, patches, rings, and square loops. The antenna with optimized dipole PRS is simulated for bandwidth increment.

R. Sauleau, et. al. [3] have presented a new configuration of low-profile, low cost, compact and directive antenna operating in V-Band. The structure comprises of microstrip patch antenna with two semitransparent mirrors (2D inductive metal meshes with square geometry and other with non-uniform grating). They concluded that the use of non-uniform metal mesh as an output reflecting surface contributes to the increasing directivity of the radiator. The radiation characteristics of Non-Uniform Gaussian Beam Antennas (NU-GBA) and the Gaussian Beam Antennas (GBAs) based on plano-convex Fabry-Perot cavities are similar and have low sidelobe level with efficiency lying between 15 dB and 23.5 dB in 60GHz band. The GBA fed by horn antenna and microstrip patch antenna is designed with non-uniform grid metal for improved performance in the directivity of antenna. The proposed design can be considered for use in WLANs.

S. A. Muhammad, et. al. [4] proposed a small-size shielded metallic stacked FPC antenna for space application. The paper proposes three different designs:

I. Single-stage Fabry-Perot cavity antenna- Structure consists of a circular waveguide with frequency selective surface (FSS) at a distance of approximately half wavelength from the waveguide aperture.

II. Stacked Fabry-Perot cavity antenna- The design comprises of waveguide fed Fabry-Perot configuration with two frequency selective surface (FSS) layers to reduce the effects of higher orders modes. The improvement was observed in the performance of directivity and impedance matching bandwidth when compared to a single-stage FPC antenna.

III. Stacked Fabry-Perot cavity antenna with corrugations- The design comprises of waveguide fed Fabry-Perot configuration with two frequency selective surface (FSS) layer and circular corrugation added in the upper layer to reduce the sidelobe level, backward radiation, and stop the propagation of surface waves.

The designs were tested in terms of directivity, gain, aperture efficiency, sidelobe level, and cross-polarization. Simulated and measured results of these designs were compared with the horn antenna.

Q. Chen, et. al. [5] have proposed a novel design of parabolic shape superstrate used as PRS to improve gain and bandwidth of Fabry-Perot resonator antenna (FPRA). The antenna is designed to operate at 6 GHz. The antenna comprised of a circular waveguide, a parabolic shaped metallic superstrate, and a ground plane. Due to the parabolic shaped superstrate, there are variations in resonance height which satisfies the resonant condition for FPRA of wideband frequency. The results of the proposed FPRA were compared with traditional planar superstrate and a significant improvement in 3-D gain bandwidth was observed from 6% to 22% for Fabry-Perot antenna with parabolic shaped PRS.

O. Ronciere, et. al. [6] proposed a Fabry-Perot antenna with rectangular waveguide for X-band along with PEC walls and metallic grid used as PRS. The paper investigates radiation characteristics, maximum directivity, aperture efficiency, and radiation bandwidth of an antenna with various configurations:

(i) Antenna with no grid and no PEC walls,

(ii) Antenna with PEC walls only, and

(iii) Antenna with grid and PEC walls.

It was observed that the radiation characteristics are a function of the size and reflectivity of PRS. The characteristics of the designed antenna were compared with large Fabry-Perot antennas and it underlines few features to take into account while designing:

(a) there exists a particular value of reflectivity for maximum aperture for any antenna size, and

(b) the resonant frequency increases by reducing the size of the shield resonator.

Ph. Coquet, et. al. [7], investigated the radiation characteristics of millimeter-wave GBA. The antenna structure comprises of a pyramidal horn antenna with a square aperture as a feed and a fused-quartz plano-convex mirror at a distance of half-wavelength. The paper

claims to give good efficiency (>50%) with very low sidelobe level(<-35dB) and low cross-polarization(<-28dB). They have designed the antenna for the mobile terminal and its efficiency depends on the reflectivity of its semi-transparent mirrors.

N. Guerin, et. al. [8] reported the design of Fabry-Perot antennas operating at 14.80 GHz with a square patch antenna used as an excitation source and Fabry-Perot cavity made up of copper grid and a ground plane. A code was developed based on the MoM to calculate the field emitted by antenna and parameters of mesh were optimized to obtain high directivity. Optimization was done in two steps:

(I) determination of propagation properties of the cavity and

(II) estimation of directivity and cross-polarization of the antenna.

Y. Ge, et. al. [9] have used partially reflecting surface with a positive reflection phase gradient for the EBG resonator antenna. The paper proposes a design of single dielectric slab PRS with printed patterns on both sides to minimize the thickness and simplify the fabrication process. It uses a monopole antenna for the excitation of the cavity. The most crucial attribute while designing the PRS is its reflection co-efficient magnitude which affects the performance of an antenna. It proposed a wideband low profile EBG resonator antenna with PRS thickness 1.6mm, the effective bandwidth is 12.6%, peak gain is 16.2dBi at 11.5GHz and 3dB gain bandwidth is 15.7%.

A.R. Wiley, et. al. [10] has presented FPA with Woodpile EBG material used as PRS and a metal ground plan. The property of complex woodpile EBG material was being investigated and was used to create a highly directional radiation pattern. The paper underlines two different antennas used as feed for FPAs: microstrip patch antenna and double slot. From the comparison between two configurations, it can be concluded that double slot feed has an advantage over patch antenna in terms of the sharp resonance due to poor reflection coefficient at the operating frequency, whereas patch antenna has the

advantage of simple and compact structure. The antenna offers high gain, efficiency, low sidelobes, and low height.

C. Cheype, et. al. [11] have studied the property of EBG material and designed an EBG resonator antenna with the use of dielectric EBG rods. The designed antenna uses dielectric EBG rods as PRS, a metallic ground plane, and a patch antenna for excitation. EBG material is a periodic structure made up of dielectric, metallic, or combination of both. They have briefly described the property of EBG material in frequency and space domain. The study in frequency domain suggests that the frequency bandgap of a material can be varied by the size and value of dielectric cells. Space domain was studied to understand the effect of material on a phase of an electromagnetic wave which allows the selection of the direction of propagation of waves. A significant improvement was observed in the gain of an antenna with low sidelobe level and excellent circular polarization.

Y. Ge, et. al. [12] have proposed a design of FPA with a thin PRS layer for wideband and low-profile EBG antenna. A single dielectric slab was used as PRS with printed dipoles on both sides. This made the design more compact and thinner compared to multiple layers of dielectric slabs used to improve the performance of antenna in the past. The designed antenna with PRS was simulated and the bandwidth of an antenna was improved with decrease in peak gain.

Based on the literature survey, it is clear that very limited research work has been carried out in the area of improving the gain of a horn antenna using Fabry-Perot Cavity (FPC). Fabry-Perot Antenna (FPA) offers+ advantages in terms of low complexity, high radiation efficiency, and a good radiation pattern. Thus, there is a need for further investigation of the FPC concept with horn antenna for different feed structures, such as rectangular, conical, corrugated, etc. The present thesis work is focused on designing a Fabry-Perot Horn Antenna with different horn configurations (pyramidal, conical, cluster of conical horns) as a primary radiator and the advantages it can offer compared to conventional horn antennas.

1.4 ORGANIZATION OF THESIS

There are altogether four chapters, including the present chapter compiled in this thesis. The thesis is organized as

Chapter-1 (Introduction) includes an overview of the topic selected for the thesis work. It discusses the motivation behind the chosen topic followed by the problem statement described for clarity of the agenda. It discusses the literature survey carried out throughout the project timeline, and lastly, the thesis organization is described.

Chapter-2 (Fabry-Perot Horn Antennas) describes a theoretical explanation of horn antenna, their type, and design procedure to be followed. It describes an overview of Fabry-Perot Antennas with an introduction, historical background behind their development, followed by some analytical models and basic types of FPAs. It also briefs about the concept of partially reflecting surfaces and the various types of material that have been used throughout the development of FPAs. Further, it includes a brief about the cluster of horn antennas used as a feed with reflector antenna for space-borne communications.

Chapter-3 (Results and Discussions) describe the simulation results carried out throughout the semester for gain enhancement of horn antenna. It depicts the design and simulation results of a circular waveguide, pyramidal horn, conical horn, and cluster of conical horn antennas with and without the partially reflecting surface. An extensive parametric study is being carried out for the final proposed design discussed at the end of the chapter.

Chapter-4 (Conclusion and Future Scope) discusses the outcome of the designed antennas and also lists out the advantages and disadvantages of designed horn antennas with FPC. The chapter ends with the future scope for working ahead.

CHAPTER-2

FABRY-PEROT HORN ANTENNAS

This chapter presents a theoretical explanation of horn antenna, their types, and designing procedure. It describes an overview of Fabry-Perot Antennas (FPAs) with an introduction, historical background behind their development, followed by some analytical models and basic types of Fabry-Perot Antennas. It also briefs about the concept of partially reflecting surfaces (PRS) and the various types of material been used throughout the development of FPAs. Further, it includes a brief about the cluster of horn antennas used as a feed with reflector antenna for space-borne communications.

2.1 HORN ANTENNAS

An aperture antenna consists of some sort of opening through which the electromagnetic waves are radiated to free space. There are three main types of aperture antennas: open-ended waveguide, horn, and slot antenna. Horn antennas are simply open-ended waveguides with flaring. The overall performance of a horn antenna depends on the type, direction, and amount of flaring given at the aperture end. It is one of the most commonly used aperture antennas. The wave travels through a guiding structure to the aperture and is radiated in free space to produce a directive beam. The amount of wave being radiated depends on the impedance matching between aperture and free space.

If we look through the development of horn antennas, the first idea was surfaced in the year 1800s by an Indian researcher Sir Jagdish Chandra Bose. In the year 1895 and 1897, Bose used circular waveguide as well as pyramidal horn antenna for investigating polarization properties of crystals. During the early 1930s, the concept of horn antenna gained popularity due to the services it provided in Second World War in the field of communication and radar. Since then numerous articles and papers are being published discussing their properties and applications in many fields.

Horn antennas are extensively used in the area of satellite tracking, communication dishes, radio astronomy, as a feed for reflectors and lenses, as a common element in phased arrays,

as a standard for calibration and gain measurements in laboratories for other high gain antennas and as medium-gain antennas.

While designing a horn antenna, there are several general properties a designer needs to consider whatever maybe the application. For instance, the radiation pattern of an antenna which includes information about the degree of sidelobe level, beam-width, cross-polarization level, directivity, front-to-back ratio, gain, phase center, and main beam efficiency. Directivity of an antenna describes how well an antenna radiates or directs the energy in a specific direction. The gain of an antenna accounts for the amount of energy radiated in a specific direction compared to the energy radiated by an isotropic antenna in the same direction when driven with the same input power.

Another electromagnetic property considered while designing a horn antenna is return loss or miss-match by their flared-out waveguide geometry. Horn antenna can be classified as shown in Fig. 2.1

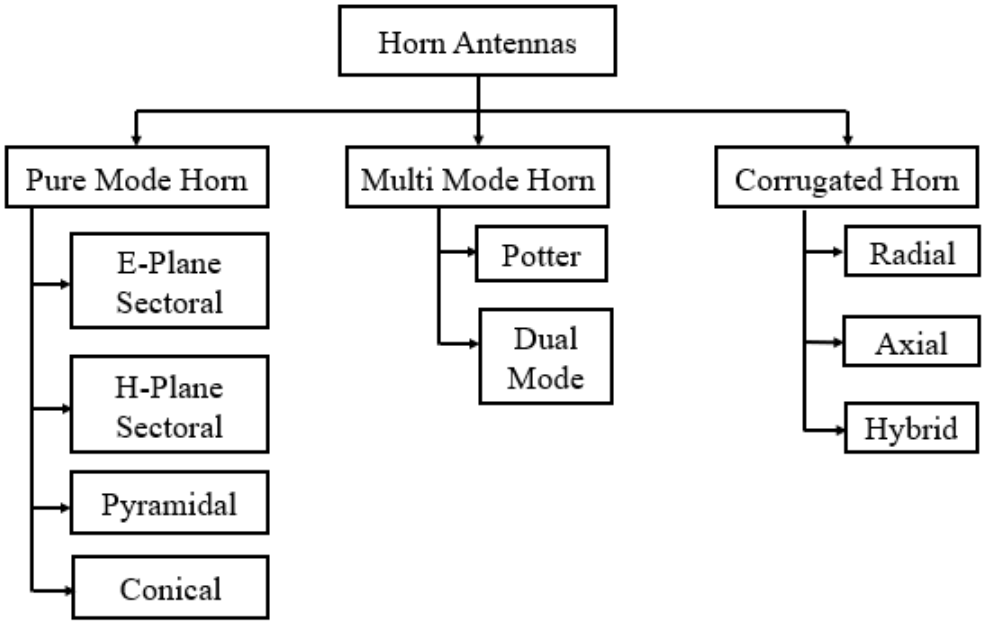

Fig. 2.1 Classification of Horn Antennas

An electromagnetic horn antenna can take many forms depending upon the types, direction, and flaring given to the structure. There are four types of pure mode horn antenna-

I. E-Plane Sectoral Horn

Horn antenna with flaring in the direction of E-field is known as E-Plane Sectoral horn antenna. The geometry is shown in Fig. 2.2.

II. H-Plane Sectoral Horn

Horn antenna with flaring in the direction of H-field is known as H-plane Sectoral horn antenna. The geometry is shown in Fig. 2.3.

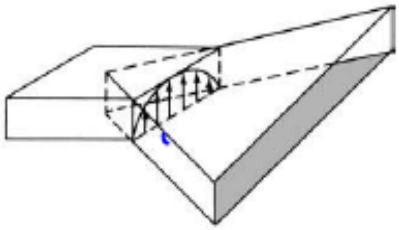

Fig. 2.2 E-Plane Horn Antenna [13]

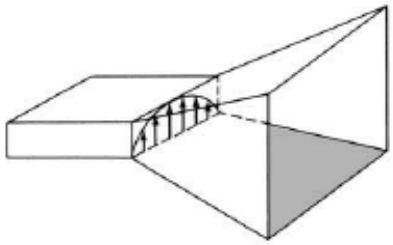

Fig. 2.3 H-Plane Horn Antenna [13]

III. Pyramidal Horn

A rectangular waveguide when flared in both directions provides a better transition between waveguide and free space and directive radiation pattern. It is known as pyramidal horn antenna. They are the most widely used horn antenna since its radiation pattern is the combination of E-field and H-field. A rectangular waveguide has TE_{10} as a fundamental mode, when it reaches the flare, to satisfy the boundary condition, it expands forming a cylindrical wave. Pyramidal Horn antennas are widely used as a standard horn antenna for the gain measurement of other antennas. The geometry of a pyramidal horn antenna is shown in Fig. 2.4

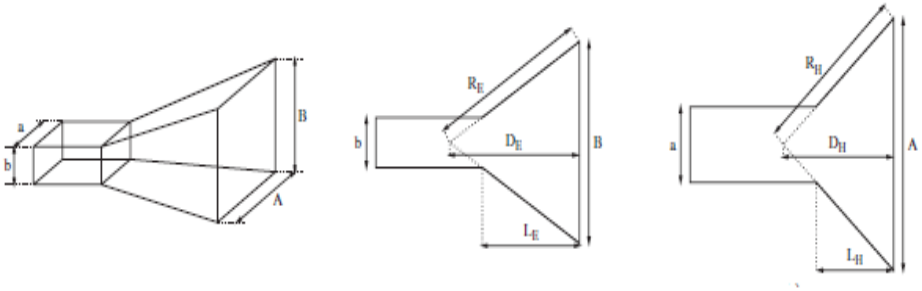

Fig. 2.4 Geometry of Pyramidal Horn Antenna [13]

The design commences with the desired gain (at first given in dBi and converted to a dimensionless quantity for calculations), design frequency, and choosing an appropriate input rectangular waveguide. A list of dimensions of rectangular waveguide is made available by the manufacturer for a specified frequency band. The procedure to be followed for designing a pyramidal horn antenna is as follows:

Note: All the dimensions are expressed in meters.

$$G_l = 10^{G_{dBi}/10} \tag{2.1}$$

$$A = 0.096aG_l^{0.232} + 0.42\lambda G_l^{0.503} - 0.193b \tag{2.2}$$

$$R_H = A\sqrt{\frac{1}{4} + \left(\frac{A}{3\lambda}\right)^2} \tag{2.3}$$

$$L_H = (A - a)\sqrt{\left(\frac{R_H}{A}\right)^2 - \frac{1}{4}} \tag{2.4}$$

$$D_H = \sqrt{{R_H}^2 - \left(\frac{A}{2}\right)^2} \tag{2.5}$$

$$B = \frac{1}{2}\left[b + \sqrt{b^2 + 8L_H\lambda}\right] \tag{2.6}$$

$$R_E = \frac{B}{2}\sqrt{1 + \left(\frac{B}{\lambda}\right)^2} \tag{2.7}$$

$$L_E = (B - b)\sqrt{\left(\frac{R_E}{B}\right)^2 - \frac{1}{4}} \tag{2.8}$$

$$D_E = \sqrt{{R_E}^2 - \left(\frac{B}{2}\right)^2} \tag{2.9}$$

Equations (2.2-2.5) are for H-field direction and Equations (2.6-2.9) are for E-field direction.

A = Width of the aperture in the H-field direction

L_H = Slant length of the aperture in the H-field direction

R_H = Half subtended angle length in the H-field direction

D_H =Axial length from apex to Center of aperture in H-field direction

B = Width of the aperture in the E-field direction

L_E = Slat length of the aperture in the E-field direction

R_E = Half subtended angle length in the E-field direction

D_E = Axial length from apex to Center of aperture in E-field direction

Ⅳ. Conical Horn

A conical horn antenna finds its widespread use in communications, radio, and radar astronomy as feed for large reflectors and lenses because of their geometrical symmetry and low cross-polarization. Flaring is given to a circular waveguide to produce highly directive beams in the desired direction. The fundamental mode of operation for the circular waveguide is TE_{11}. The basic geometry of the conical horn antenna is shown in Fig. 2.5.

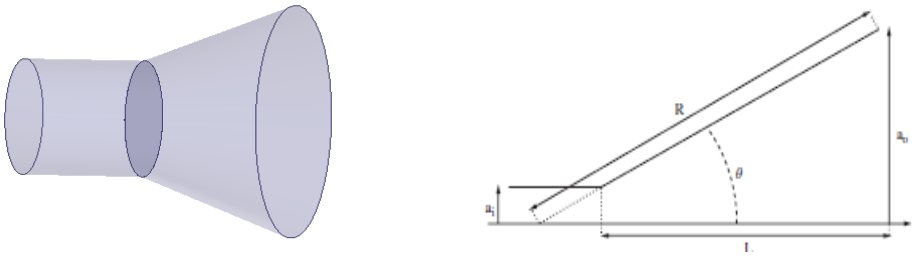

Fig. 2.5 Geometry of Conical Horn Antenna [13]

To design a conical horn antenna for a specific design frequency and gain the following procedure is to be considered.

Note: All the quantities are expressed in meters.

$$a_i = \frac{3\lambda}{2\pi} \tag{2.10}$$

$$a_o = \frac{\lambda}{2\pi}\sqrt{10^{(G_{dBi}+2.91)/10}} \tag{2.11}$$

$$R = \frac{4{a_o}^2}{3\lambda} \tag{2.12}$$

$$\theta = arcsin\frac{a_o}{R} \tag{2.13}$$

$$L = \frac{a_o - a_i}{tan\theta} \tag{2.14}$$

Here,

a_i=Input radius

λ=wavelength

a_o= Output radius

R= Half subtended angle length

L=length of horn

Θ=Half Subtended angle

2.2 FABRY-PEROT ANTENNAS

2.2.1 Introduction

Based on the principle of superposition of waves, in the year 1899 Charles Fabry and Alfred Perot developed a concept of Fabry-Perot Interferometer (FPI). FPIs are an optical cavity that consists of two parallel mirrors which partially transmits and reflects the wave incident on it and these waves are focused on screen to produce an interference pattern. The incident light is partially reflected and transmitted multiple times, each time splitting the wave amplitude infractions, and phase change of half-wavelength. The light waves incident on the mirror is separated into two fragments, where the smaller fragment is transmitted through the second mirror and the larger fragment is reflected between the cavity allowing plenty of subsequent reflections and transmissions. This produces an interference pattern on the screen placed at some distance in front of the mirror. The pattern includes a constructive and destructive interference of waves producing a bright and dark band respectively on the screen. Fabry-Perot interferometers find a wide range of applications in telecommunication, spectroscopy, and astronomy. The principle of FPI is depicted in Fig. 2.6

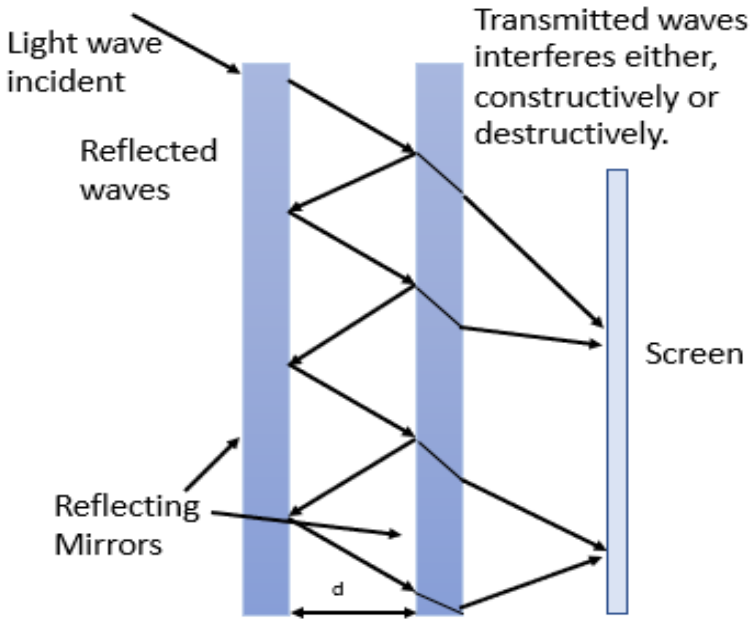

Fig. 2.6 Working Principle of Fabry-Perot Interferometers (FPI)

The interference pattern produced on the screen depends on the distance between two screens and can be altered as per applications. The interference pattern is produced due to the path difference which is given as

$$Path\ Difference = m \times \lambda \quad (2.15)$$

$$Path\ Difference = 2 \times d \times \cos\theta \quad (2.16)$$

Here, d is the distance between two mirrors,

λ is the wavelength of the incident light,

Θ angle of the incident light and m are integer numbers.

The principle of FPI when applied with antennas i.e. when a conducting screen is placed in front of an antenna it affects the performance of an antenna based on its distance from the radiating aperture providing a new area for research: Fabry-Perot Resonator Antennas (FPRAs) or Fabry-Perot Cavity Antennas (FPCAs) or Fabry-Perot Antennas (FPAs). A Fabry-Perot Antenna (FPA) comprises of a partially reflecting surface (PRS) illuminated by a primary radiator (which can be a patch antenna, waveguide, or a horn antenna) backed with a metallic ground plane. The basic structure of FPAs is depicted in Fig. 2.7

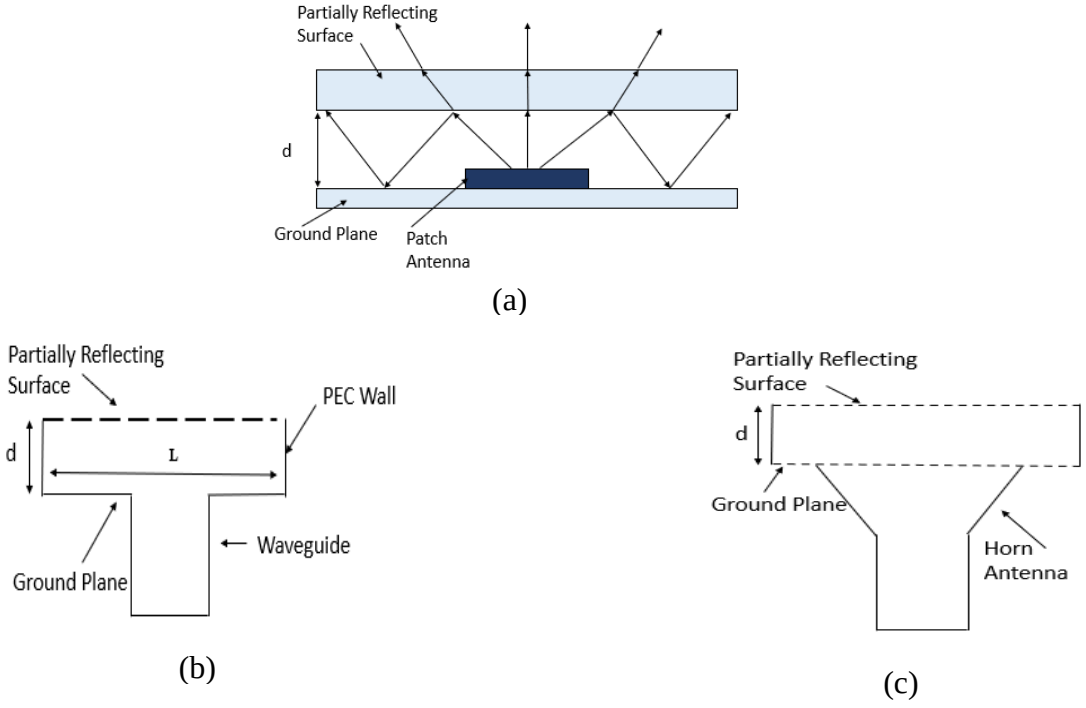

Fig. 2.7 Geometry of FPAs with (a) Microstrip Patch, (b) Waveguide, and (c) Horn Antenna as Primary Radiator

A significant improvement in the performance of the antenna is observed such as an increase in directivity, gain, radiation pattern, low complexity in structure when compared to the conventional array of antennas with a complex feeding network and high radiation efficiency due to in-phase bouncing between the two surfaces (PRS and ground plane). The gain and bandwidth of an antenna depend on the distance between the two planes and reflections from PRS.

Thus, to form a Fabry-Perot cavity, the partially reflecting surface is placed at a distance of about integer times the half-wavelength and in parallel to the ground plane. Various implementations have been proposed over several years for the type of PRS used in FPAs depending upon the application and demand. It can be formed by wires and metallic stripes or grating [1,3,5,6,8], dense quarter wavelength single [14] or multi-layered dielectric sheets [15,16,18], electromagnetic band-gap (EBG) [9-12], frequency selective surface (FSS) [4,17] and metamaterial surface.

Thus, Fabry-Perot antennas offers many advantages such as high directivity, gain, good radiation pattern, and low complexity in the structure. All these advantages in conjunction with the recent advancement in the metamaterial and periodic surface led to a reinvigoration of new research areas of the antenna. Fabry-Perot antennas find their applications in wireless communication, radar applications, and satellite communication.

2.2.2 Historical Background

The very first implementation of the Fabry-Perot antenna though the name was not coined during that period was done in the year 1956 by G. V. Trentini [1]. He described a full mathematical analysis for deriving a radiation pattern between the reflection sheet and the parallel screen. He implemented the concept using a waveguide and different types of PRS such as wires, stripes, grids, perforated sheets, and dielectric glass to enhance the directivity of the waveguide.

In the year 1985 and 1987, an independent study was done for enhancing the gain of an antenna by introducing the concept of antenna embedded on a substrate with single or multiple superstrates. It was observed that the gain of an antenna is directly proportional to the permittivity and permeability of superstrate material and bandwidth is inversely proportional to the gain of antenna which limits

its performance [14]. The performance of an antenna can be varied by changing the number of superstrate layer and its thickness [15].

Furthermore, in the year 1898 [17] a frequency selective surface (FSS) was used in front of the waveguide aperture for beamforming; it used a simple ray theory to explain the leaky waves in FSS. It compares various radiation patterns of different types of FSS configurations such as capacitive and inductive by placing at a different distance from the excitation source. It was in the year 2001 when the similarity with the principle of FPI which is used in optics was found with the operating principle of the antennas with a PRS structure placed in front of a waveguide aperture was analyzed. It concluded that the reflection characteristics of PRS and the distance between the ground plane and PRS affect the performance of the antenna. After that several papers have been published to date with a similar concept in the urge of enhancing the antenna performance for meeting the industrial requirement.

The development of FPA with PRS can be summarized as PRS made up of wires or strips/grid, single-layered dense dielectric sheet, multilayered dielectric sheet, EBG, FSS, and metamaterial. The antenna used as a primary radiator to illuminate the PRS can be a microstrip patch, a slot in the ground plane, waveguide, or a horn antenna.

2.2.3 Fabry-Perot Antenna Analysis Techniques

With all the advancements in Fabry-Perot antennas, there are several models proposed to analyze the performance of the Fabry-Perot antenna. All the analytical models described below serve different purposes, for instance, the Fabry-Perot cavity model provides a mathematical approach towards the analysis by estimating the directivity performance based on reflection characteristics of the PRS. The principle of reciprocity method reduces the estimation process of the determination of the far-field. The leaky wave model is used for determining the characteristics of a radiated beam from a complex wave number of leaky modes. Other methods considered for the analysis are electromagnetic band-gap (EBG) defect model and transmission line model which provides the formulas for resonance gain, beam-width, and bandwidth for the FPA.

The Fabry-Perot cavity model is based on geometric optics approximation to describe the mathematical operation of FPAs. This method was adopted to describe the path of transmitted and reflected waves. Consider a metallic ground plane with a reflection coefficient $r_1\angle\emptyset_1$ and PRS with a reflection coefficient $r_2\angle\emptyset_2$ with the distance of h between them. The plane wave inside these two planes goes through multiple reflections with changes in amplitude and phase of the wave.

The phase shift can be expressed as,

$$\frac{-4\pi h}{\lambda} + \phi_1 + \phi_2 = 2\pi N, \text{ N=1,2…} \quad (2.17)$$

The resonant frequency of FPA can be mathematically expressed as

$$f = \frac{c(\emptyset_1+\emptyset_2)}{4\pi h} \quad (2.18)$$

where h is cavity height. Usually, the values of the reflection coefficient $\emptyset_1 = \emptyset_2 = \pi$, and thus cavity height is equal to half wavelength, $h = \frac{\lambda}{2}$. This approach assumes an infinite size structure that gives an estimation of the directivity performance of an antenna after calculating the reflection characteristics of a PRS structure. It does not take into account the diffraction effects and higher-order mode coupling.

Another approach towards analysis of the FPA structure is the principle of reciprocity. It describes that when a source is placed at a far-field it will provoke electric field strength inside the structure, thus the far-field radiation characteristics can be estimated by calculating the field at an observation point when an antenna is illuminated by a plane wave of fixed magnitude at a various angle of incidence.

The relative electric field strength is sampled at an observation point for a different angle of incidence value to obtain the radiation pattern of an antenna. Thus, this approach reduces the need for estimating the far-field radiation pattern. It can be employed for the FPA structure with multiple periodic structures.

The third method used for FPA analysis is the leaky-wave model. The FPA structure consists of PRS that has partial transparency at the resonant frequency and related leaky-modes; hence the model can be used for their analysis. The information about leaky wave antennas can be obtained from the expression $k = \beta - j\alpha$, where the real part of k is the attenuation constant and provides an angle of the radiated main beam while the imaginary part is phase constant and gives information about bean-width.

Leaky wave antennas consist of guiding structure through which waves propagate, to analyze FPAs the structure is replaced by partially reflecting surfaces that allow leakage of waves and one can determine the radiation pattern using Green's function. This method is very tedious but provides an accurate result.

Another method that can be considered to analyze FPA is the Electromagnetic Band-Gap (EBG) defect model. A Fabry-Perot antenna can be considered as an EBG resonator antenna with a defect introduced in the periodicity of the material which allows the display of localized frequency in the forbidden gap. This improves the directivity of an antenna as the EBG material used PRS in the FPA structure introduces a disturbance in EM wave distribution and hence increases the aperture of an antenna.

The most recent method used is the Finite Difference Time Domain (FDTD) where an individual unit cell is model and analyzed. When metamaterial or metallo-dielectric FPAs are to be analyzed this method provides an accurate result as it allows computationally efficient calculation of electromagnetically converged waves.

2.2.4 Basic Types of Fabry-Perot Antennas

Fabry-Perot Antennas are differentiated on the grounds of the material used for partially reflecting surface. They are classified into three categories: metallic, dielectric, and metallo-dielectric Fabry-Perot antennas.

I. Metallic Fabry-Perot Antennas

When the PRS considered in the Fabry-Perot is purely metallic they are classified as metallic FPAs. The metallic PRS can be a perforated sheet or metallic strip grating placed at a particular distance to enhance the antenna performance in terms of gain, directivity, beam control: reconfiguration, or shaping. There are several papers published with the all-metallic structure of the FPC antenna, for instance, in [3] a perforated metallic sheet is designed to improve the gain of an antenna operating in V-band. It consists of a thick perforated metallic FSS sheet placed in front of a waveguide aperture. It was concluded that the performance of FPA depends on the thickness, shape, size, and periodicity of holes in the sheet.

The performance of FPAs with metallic PRS depends on the reflectivity and distance between the ground plane and PRS. The reflectivity of the grid depends on the dimensions and the spacing between the grids. For perforated sheets, the reflectivity depends on the shape of the holes (square, dipole, or circular), size, and the periodicity.

The excitation source can be microstrip patch antenna, metallic waveguide as shown in Fig. 2.8(a) and horn antenna as shown in Fig. 2.8(b). In [19-20] a detailed parametric study is carried on 60GHz Fabry-Perot antenna by varying the dimensions of metal meshes used as PRS for the analysis of their effect on the radiation performance of an antenna. Furthermore, [4] and [21] describes a metallic stacked Fabry-Perot antenna for large bandwidth and circular polarization respectively intended for space applications. Both the papers use frequency selective surface as partially reflecting surface.

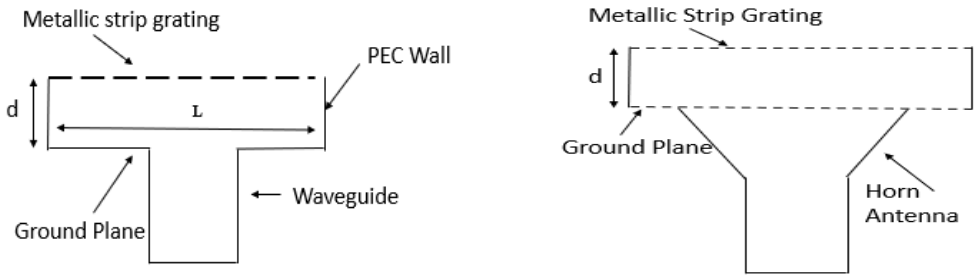

(a) 1 (b)

Fig. 2.8 Metallic Strip Grating as PRS with (a) Waveguide and (b) Horn Antenna as Primary Radiator.

II. Dielectric Fabry-Perot Antennas

The Fabry-Perot antennas with a dielectric layer (single or multiple) used as PRS were investigated in the mid-1980s [14-17]. In [14] the authors have used a single layer dielectric superstrate for gain enhancement placed in front of a substrate with a Hertzian dipole embedded in it. The concept of multiple layer superstrates for gain enhancement method was introduced in [15]. The single layer and multi-layered dielectric superstrate are depicted in Fig. 2.9.

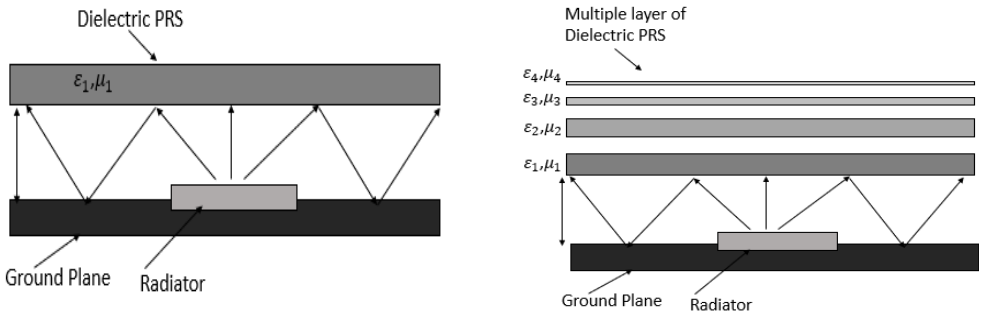

(a) (b)

Fig. 2.9 Geometry of FPAs with (A) Single Layer, and (B) Multi-Layer Dielectric as PRS.

The reflection characteristics of PRS are the most critical parameter to maintain as the operation of FPAs depends on it. And the reflection characteristics of PRS depend on the magnitude of the reflection coefficient which is the function of the dielectric constant of the material, the thickness of the layer, permittivity value, and reflection coefficient. Thus, the reflection characteristics can be altered by varying dielectric constants, altering the thickness of the layer, different permittivity values, and multiple layers of dielectric sheets with variations in their thicknesses, distance from the ground plane. The high directivity is achieved by using a large number of layers, but this comes with a drawback of narrow bandwidth and reduces the degree of freedom in designs. There are several papers [9-12, 21-23] which describe the use of dielectric layer as PRS for enhancing gain and directivity of an antenna.

III. Metallo-Dielectric Fabry-Perot Antennas

The Fabry-Perot antennas with PRS structured with metallic patches embedded on a dielectric slab is defined as Metallo-dielectric FPAs. The basic geometry of these types of antennas is shown in Fig. 2.10

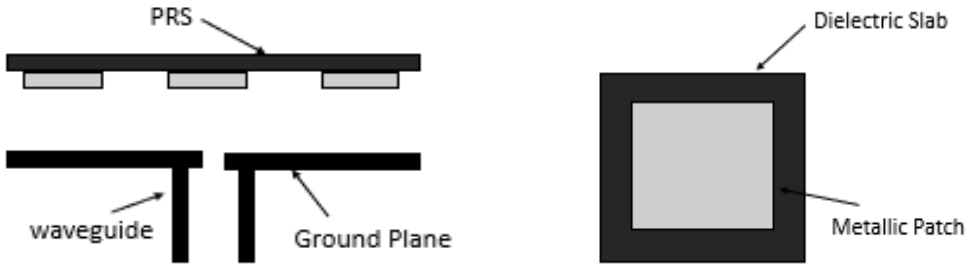

(a) (b)

Fig. 2.10 Geometry of FPAs with (a) Metallo-dielectric PRS and (b) Front view of PRS

Many papers are being published on this type of antenna for bandwidth enhancement [9, 12, 24-28], low profile antennas [9, 29], beam focusing [30], and enhancement in directivity, and gain [31-34]. In [31] the PRS is designed for high gain antenna using a dielectric slab with squared shape copper patch array embedded on it. The PRS was designed to investigate the directivity of a patch antenna used as a fed to PRS. It was concluded that the gain and directivity of an antenna depend on the reflection coefficient of PRS, cavity height, a cross-section of PRS. And the reflection co-efficient of PRS was varied by changing the patch length. To overcome the narrow bandwidth limitation of EBG material, several attempts were made. However, in [9] PRS with single-layer dielectric and printed dipoles on both the side is proposed to provide a wideband EBG resonator antenna.

2.2.5 Partially Reflective Surface

A surface or sheet made up of any material capable of partially reflecting and transmitting electromagnetic waves when incident on it are known as partially reflective surfaces (PRS). It possesses the capability of increasing the aperture efficiency of an antenna. It was in the year 1956 when the concept of FPA was surfaced when Trentini used several types of partially reflecting surfaces to enhance the directivity of the waveguide antenna. It stated that when a conducting screen is placed behind an antenna it serves as a shield against backward radiation and also effects the forward radiation pattern depending upon the material used, the distance between the sheet and antenna, the dimensions of the PRS layer and its reflection coefficient.

A significant improvement in radiation pattern, directivity, and gain of an antenna is observed by considering all the mentioned parameters while developing a Fabry-Perot antenna. Thus, the most important attribute while designing FPA is the selection of the material and the type of partially reflecting surface. Throughout the development of FPAs, the material being explored for the use of PRS are metal wires or grids [1, 20, 35-36], a dielectric layer(s) (single or multiple) [14-18, 24], electromagnetic band-gap [9-12, 22-23], frequency selective surface [4-8, 21, 38-44] and most recent are the metamaterials.

Metal grids were used in [1] for increasing the directivity of waveguide antenna and the results were compared when grids were replaced by dielectric plate-glass. The paper suggests that all forms of PRS can be used. In the mid-1980s, dielectric material was used for gain enhancement of antenna. An electric insulator that can be polarized by an electric field is known as a dielectric material. When EM waves are incident on these types of material, they go through phase shift and change in amplitude which results in partial transmission and reflection of waves.

While designing a Fabry-Perot antenna with a dielectric sheet as PRS one must consider the dependency of gain and directivity on the reflection characteristics of PRS, which is directly proportional to the dielectric constant. For high gain and directivity, high reflectivity is required from the PRS layer. Reflectivity of the dielectric layer can be increased by increasing the thickness of the sheet or increasing the number of layers of dielectrics sheet, with the variation in thickness of layer and permittivity values. Thus, the use of dielectric superstrate may provide many advantages but reduces the degree of freedom. Many papers are being published with the use of a single layer and multi-layered dielectric sheets

Another popular material used as PRS is Electromagnetic Band-Gap (EBG), the material led to the idea of the EBG defect model used for the analysis of a Fabry-Perot antenna. EBG materials are the periodical structure which consists of dielectric or metallic elements. It has a few characteristics behavior which makes it an appropriate candidate for the use as PRS material,

1. It forbids the propagation of the electromagnetic waves whose frequency lies within their frequency bandgap. The band depends on a material structure that includes dimensions, periodicity, and permittivity.
2. By introducing a few defects in the periodical structure one can open a localized electromagnetics mode inside the forbidden frequency band. It is one of the most important characteristics of EBG material as one can change the frequency bandgap of the material by introducing a defect which can help in choosing the desired frequency.

There are many applications in which EBG material is used. For example, in an optical domain where they are used to develop high-quality mirrors or micro-cavities, in the electromagnetic domain they are used to realize waveguide and frequency filters. They are also used as an antenna substrate to provide mechanical support for an antenna. With the recent advancement in material such as FSS and metamaterials composed of uniform and non-uniform unit cells also considered as an appropriate candidate to form the PRS layer.

2.2.6 Frequency Selective Surface

Frequency Selective Surface (FSS) is a type of meta-surfaces that merely exhibits an electric response. They are periodic surfaces composed of an array of metallic holes or patches, or an array of a two-dimensional element embedded on a dielectric substrate. When the frequency of incoming EM waves resonant with the frequency of FSS element, the waves are either transmitted or reflected completely or partially depending on the nature and types of elements used. The resonance depends on element size, shape, and periodicity. They find applications ranging from diplexers for microwave devices, resonance beam splitter, as antenna radomes, and controlling radar cross-section. Some of the desired properties of FSS are low profile, reduced periodicity, dual-polarization, angular stability, and easy manufacturability. They are also known as spatial filters.

The operating principle of FSS can be described as when EM waves are incidents on structure, they generate an electric current into array elements that work as EM sources which produce a scattered field which when combined with electric field make up the resultant field around the FSS structure. There are three types of FSS element groups. A few of them are depicted in Fig. 2.11

- Group A: Dipole, tripole, square-spiral, Jerusalem crosses

- Group B: Patches of different shapes like square, circular and hexagonal
- Group C: Loop shapes like circular, square, hexagonal

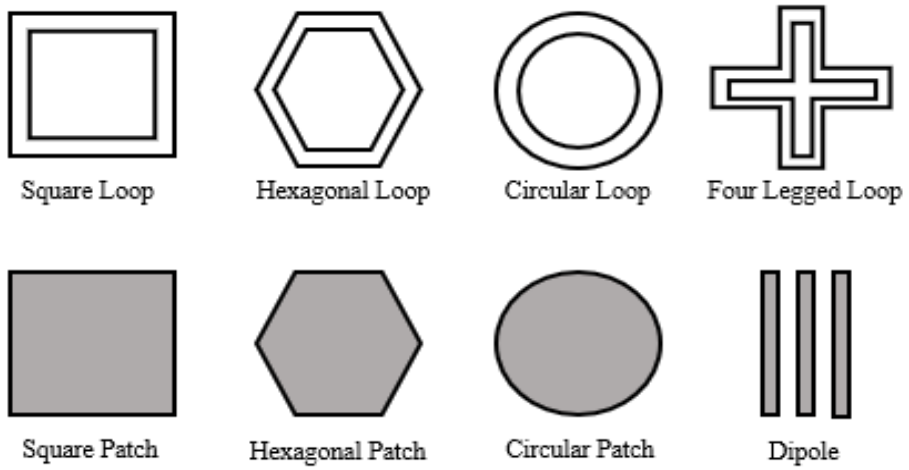

Fig. 2.11 Different Configuration of Frequency Selective Surface (FSS)

The bandwidth is inversely proportional to the inter-element spacing and at a certain closer distance the capacitance of inter-element increases which shifts the resonance frequency towards the lower band. Thus, for a desired resonant frequency and bandwidth the circumference of the element is to be reduced. Conventionally, FSS reaches the desired resonance frequency when the patch or slot size is equivalent to half of the wavelength. Thus, for desired resonant frequency and bandwidth miniaturized elements were proposed with small metallic arrays like metallic patches (capacitive) and wire grids (inductive) as shown in Fig. 2.12. There are several papers [4, 21, 33-34, 38-44] which describes the use of FSS as PRS for enhancement of antenna performance.

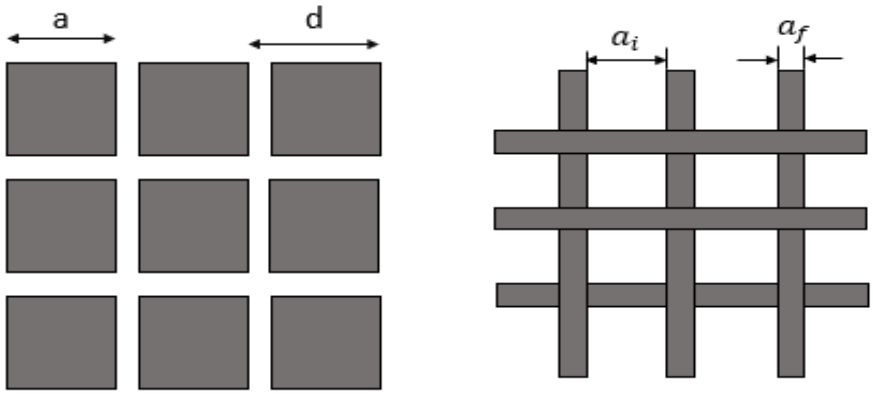

(a) (b)

Fig. 2.12 Geometry of FSS (a) Metal Patch and (b) Metal Grid

2.3 CLUSTER OF HORN ANTENNAS

Reflector antennas due to their higher directivity when illuminated by small feeds are generally used for transmission and reception of RF signals by communications satellites to communicate to Earth stations. Reflector antennas are illuminated by a feed (directly or indirectly through sub-reflector) to provide gain coverage over a specific region on Earth. Thus, the feed of reflector is important hardware for satellites. It defines bandwidth, power handling, passive intermodulation levels, and illumination on reflectors. There can be single or multiple feeds to provide beam coverage over a specific area.

Horn antennas are widely used as feed for reflector antennas. The radiation pattern of a single antenna element generally provides a wide radiation pattern with low directivity and gain, but for long-distance communications, it is necessary to have high gain antennas. There are two distinct methods to increase the gain of horn antenna it includes increasing the aperture size of the antenna which in turn increases the directivity and gain of gain. However, there are many applications where the size and weight of antenna are predefined. Another method is forming an array of individual horn antenna without increasing the size of an individual element.

An antenna array consists of a set of identical radiating elements organized in a specific manner to obtain the desired radiation pattern. An array can be formed of two or more individual elements. Each element in the array is designed to have an identical radiation property. The total field of an array is determined by vector addition of the fields radiated by individual elements. In an array of an identical element, the overall radiation pattern can be controlled by

a) the geometrical configuration of an overall array (cluster of horn antennas can be formed 1-, 3- and 7-feed horn design),
b) the relative displacement between these individual elements,
c) the excitation amplitude and phase of an individual antenna, and
d) the individual radiation patterns.

Different configurations of feed clusters are depicted in Fig. 2.13. The illuminating feeds for reflector are conical horn antennas. The concept of array of antenna or cluster of feed antennas is important to fulfill the objectives such as gain enhancement for satellite communication, beam

steering, and to find the direction of arrival for radar systems, antenna diversity for mobile phones, to improve S/N ratio for the satellite receiver.

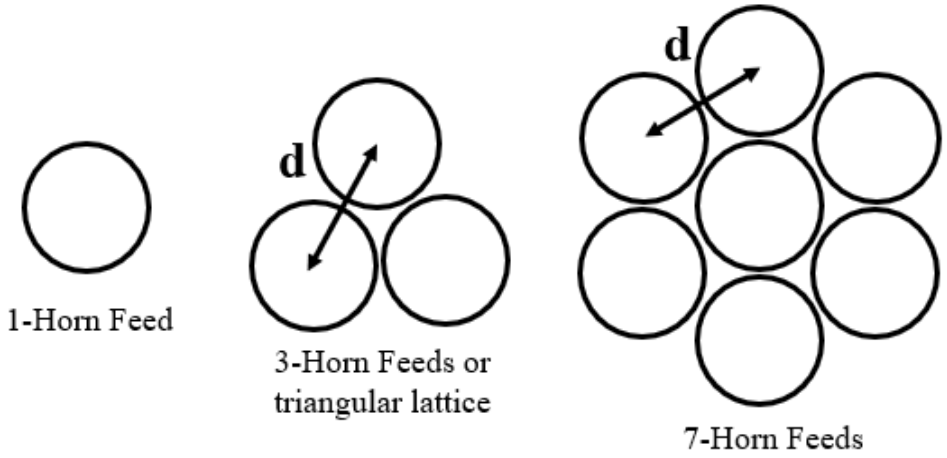

Fig. 2.13 Different Configurations of Feed Clusters

CHAPTER-3

RESULTS AND DISCUSSION

This chapter includes a description of the designed Fabry-Perot horn antennas and a discussion of their simulated results. All the designs are simulated in High-Frequency Structure Simulator-HFSS v.2014 [50]. For all the design described, an extensive parametric analysis is performed to get the best results. The chapter is divided into four sections as follows:

- Implementation of a circular waveguide with and without partially reflecting surface.
- Design of a pyramidal horn antenna with and without partially reflecting surface.
- Design of a conical horn antenna with and without partially reflecting surface.
- Design of a cluster of conical horn antennas with and without partially reflecting surface.

3.1 IMPLEMENTATION OF A CIRCULAR WAVEGUIDE USING PARTIALLY REFLECTING SURFACE

A circular waveguide with PRS is implemented and described in this section. The section is divided into three parts with design variations as follows:

1. Single-Stage Fabry-Perot cavity antenna
2. Stacked Fabry-Perot cavity antenna
3. Stacked Fabry-Perot cavity antenna with Corrugation

Designs presented here are analyzed in terms of return loss, directivity, and gain. A comparison is presented between reference and simulated values of each design.

3.1.1 DESIGN-1: SINGLE-STAGE FABRY-PEROT CAVITY ANTENNA

The geometry of a single-stage Fabry-Perot cavity antenna is shown in Fig 3.1. It consists of a circular waveguide, a metallic ground plane, and a frequency selective surface (FSS) as a PRS placed at a distance above the ground plane. An inductive gird is used rather than a capacitive grid, to avoid the use of dielectric material as a substrate. The mesh period and strip width of the grid is labeled as a_f and d_f respectively. A circular waveguide comprises

an iris and a waveguide penetration for impedance matching. The dimensions of the single-stage FPC antenna and metallic FSS inductive grid are given in Table 3.1.

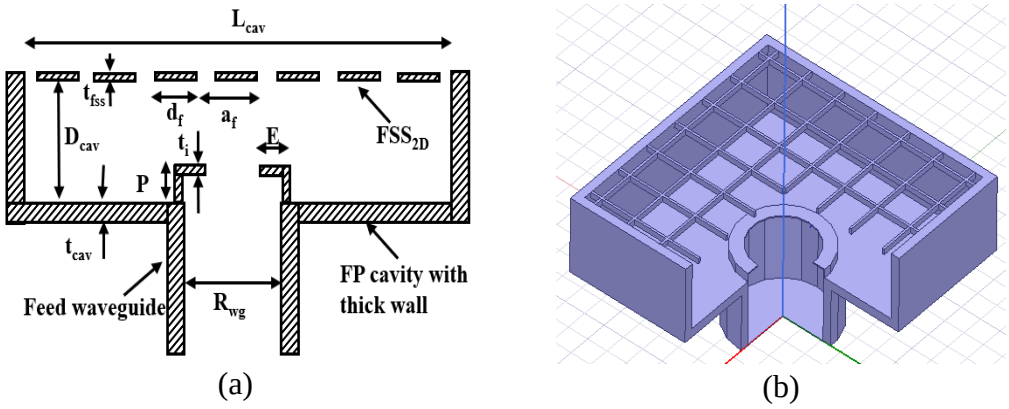

Fig. 3.1 Geometry of a Single Stage FPC antenna (a) Schematic View and (b) 3D Model

Table 3.1 Dimensions of Single Stage Fabry-Perot Cavity Antennas

Antenna Aperture	$L_{cav} = 223\ mm \times 223\ mm$
Cavity Height	$D_{cav} = 56\ mm$
Feed Waveguide	$R_{wg} = 85\ mm$
Antenna Waveguide Penetration and Iris	$P = 8\ mm, E = 12\ mm, T_i = 1\ mm$
Frequency Selective Surface (FSS)	$a_f = 34\ mm, d_f = 2\ mm, t_{fss} = 5\ mm$
Cavity Wall Thickness	$t_{cav} = 8\ mm$

The amount of reflection from the PRS layer depends on the distance between PRS and ground plane and the reflection characteristics of PRS. Thus, for obtaining an accurate result, the cavity height is to be tuned for a given cavity size and reflectivity value of FSS. The simulation results for return loss, directivity, and gain are shown in Fig. 3.2, 3.3, and 3.4, respectively. We obtained a close agreement between the simulated and the reference value. The design was simulated over the range of 2.4 – 2.55 GHz. The maximum gain of 15.32 dBi at 2.5 GHz with return loss < -5 dB was observed.

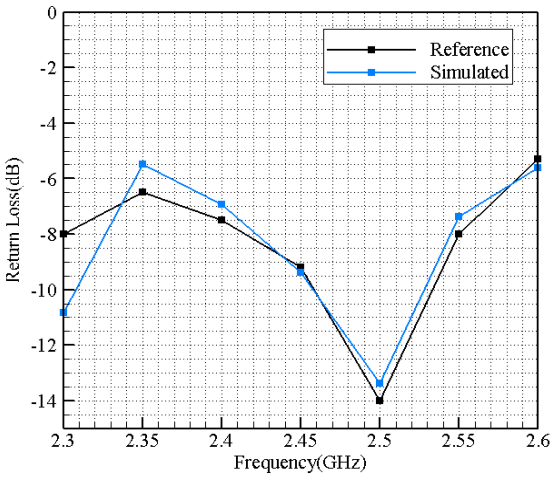

Fig. 3.2 Return Loss of a Single Stage Fabry-Perot Cavity Antenna

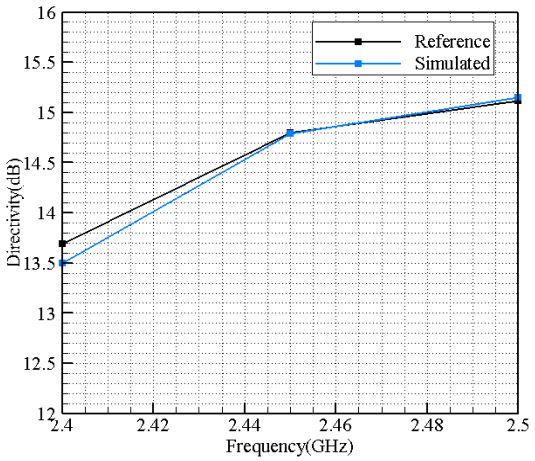

Fig. 3.3 Directivity of a Single Stage Fabry-Perot Cavity Antenna

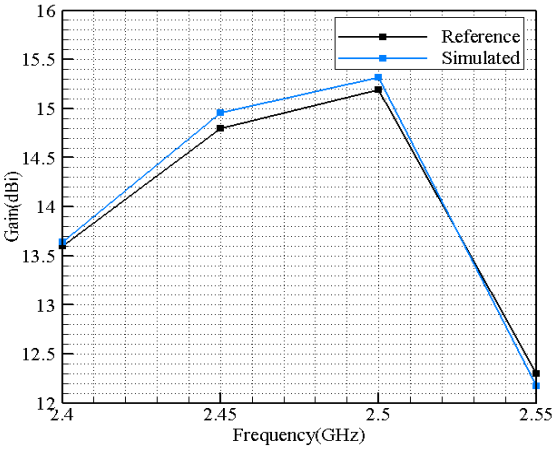

Fig. 3.4 Gain of a Single Stage Fabry-Perot Cavity Antenna

3.1.2 DESIGN-2: STACKED FABRY-PEROT CAVITY ANTENNA

The geometry of the stacked Fabry-Perot cavity antenna is shown in Fig 3.5. It consists of a circular waveguide with two-square FP cavity stacked on top of each other with the bottom cavity serving as an impedance matching intermediate stage and larger cavity as a radiating element. The main objective to introduce stacking in single-stage FPC is to reduce higher-order modes. There is no iris in stacked FPC configuration as it serves as a narrow band impedance matching for the highly reflective grid. The dimensions of the stacked FP cavity are given in Table 3.2.

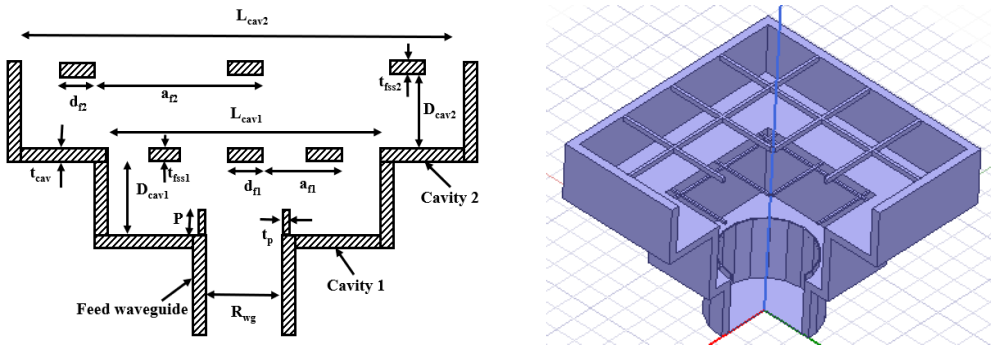

(a) (b)

Fig. 3.5 Geometry of Stacked Fabry-Perot Cavity Antenna (a) Schematic View and (b) 3D Model

Table 3.2 Dimensions of Stacked Fabry-Perot Cavity Antenna

Antenna Aperture	L_{cav1} = 121mm×121mm L_{cav2} = 223mm×223mm
Cavity Height	D_{cav1} = 68 mm D_{cav2} = 47.5mm
Feed Waveguide	R_{wg} = 85 mm
Waveguide Penetration	P = 8 mm, t_p = 1mm
Frequency Selective Surface (FSS)	a_{f1} = 52 mm, d_{f1}= 2mm, t_{fss1}= 2mm a_{f2}=52mm, d_{f2}= 2mm, t_{fss2}= 2mm
Cavity Wall Thickness	t_{cav}= 8 mm

The simulated results for return loss, directivity, and gain are shown in Fig 3.6, 3.7, and 3.8, respectively. The maximum gain of 15.23 dBi is obtained at 2.55 GHz.

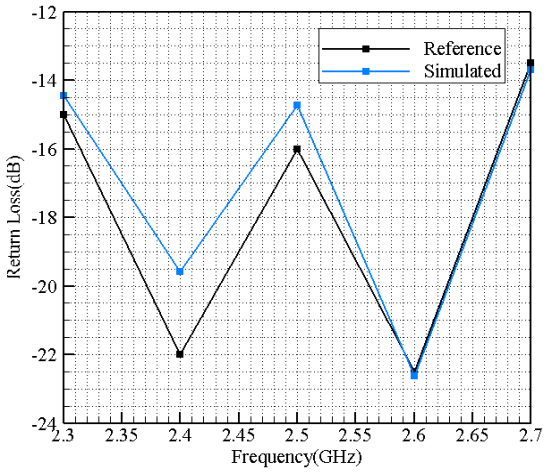

Fig. 3.6 Return Loss of a Stacked Fabry-Perot Cavity Antenna

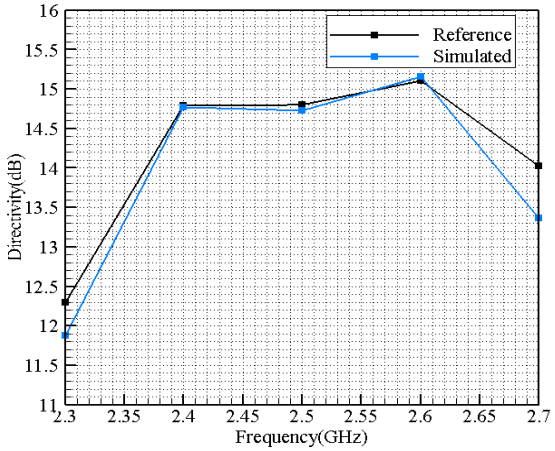

Fig. 3.7 Directivity of a Stacked Fabry-Perot Cavity Antenna

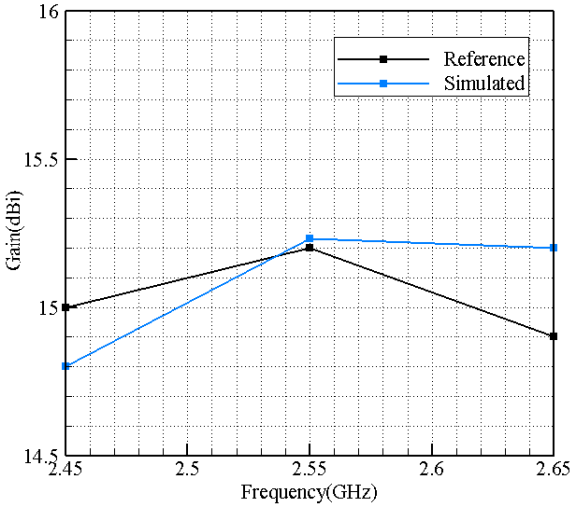

Fig. 3.8 Gain of a Stacked Fabry-Perot Cavity Antenna

3.1.2 DESIGN-2: STACKED FABRY-PEROT CAVITY ANTENNA WITH CORRUGATIONS

Corrugations are introduced in horn antennas to reduce the sidelobe levels, backward radiation, and propagation of surface-wave. They are introduced in a stacked FPC antenna in the upper cavity as it is the radiating element and are more prone to parasitic modes. The dimensions of a stacked FPC antenna with corrugation are kept the same as of stacked FPC antenna and the dimension of corrugation is optimized using the HFSS tool. Their typical size is taken as $l_c = \frac{\lambda_0}{4}, a_c \leq \frac{\lambda_0}{2}$, and $d_c \leq \frac{a_c}{2}$. The schematic diagram of a stacked FPC antenna is shown in Fig. 3.9. The dimensions of corrugation are considered after a parametric analysis in the HFSS tool. Simulated results are shown in Fig. 3.10 and 3.11.

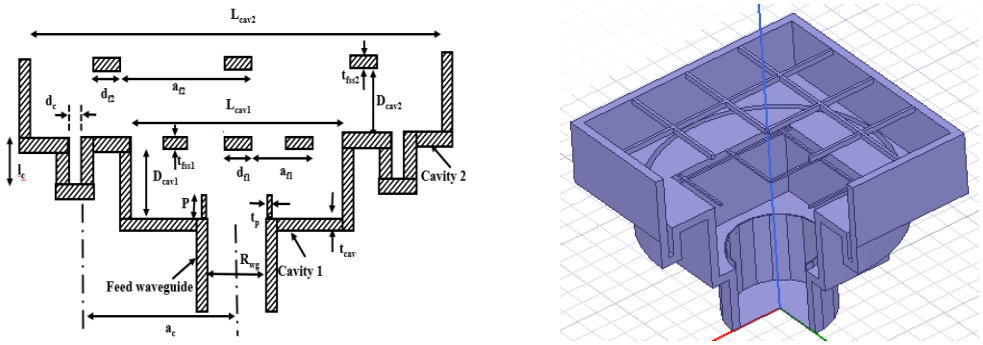

(a) (b)

Fig. 3.9 Geometry of Stacked Fabry-Perot Cavity Antenna with Corrugation (a) Schematic View and (b) 3D Model

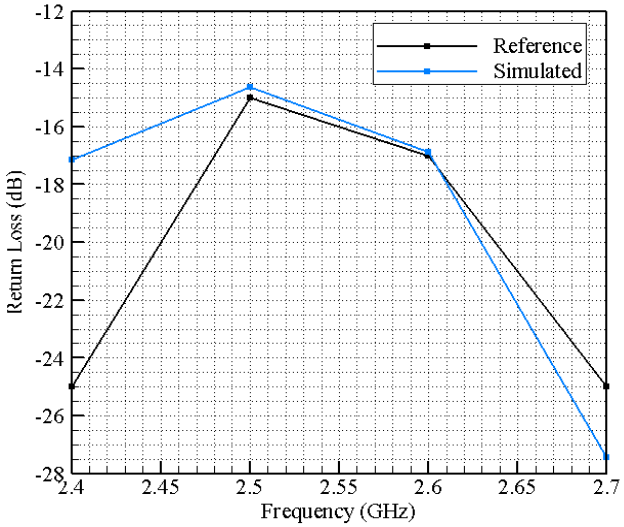

Fig. 3.10 Return Loss of a Stacked Fabry-Perot Cavity with Corrugation

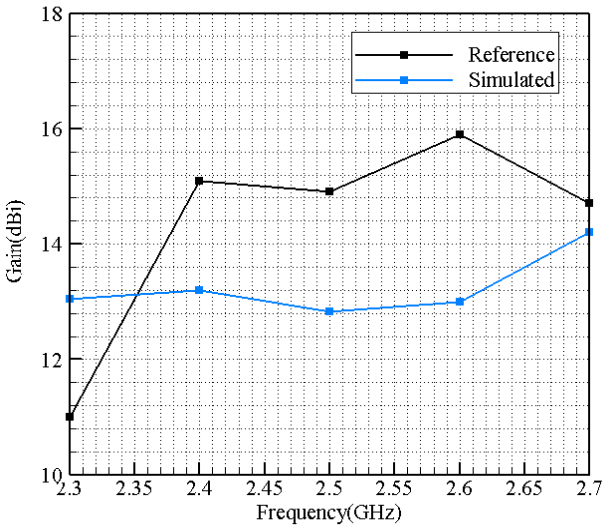

Fig. 3.11 Gain of a Stacked Fabry-Perot Cavity with Corrugations

After comparing all the three designs of Fabry-Perot antennas, it can be concluded that a single-stage FPC antenna provides a maximum gain of 15.32 dBi at 2.5 GHz and it can be used for a narrow-band application. The said design is modified by introducing,

I. Stacking of layers to reduce the effects of higher-order modes,

II. Circular corrugations to reduce the sidelobe level and propagation of surface waves.

However, these modifications can make the antenna systems bulky and complex.

3.2 DESIGN OF A PYRAMIDAL HORN ANTENNA WITH AND WITHOUT PARTIALLY REFLECTING SURFACE

A pyramidal horn antenna is designed for frequency range 2.2-3.3 GHz. The main objective is to enhance the gain of the horn antenna by applying the concept of a Fabry-Perot cavity. It is formed with three elements: a primary radiator (in this case we have chosen pyramidal horn antenna), a partially reflecting surface (a frequency selective surface i.e. an inductive metal grid) place at an appropriate distance from the antenna aperture or ground plane. The dimensions of the proposed design are given in Table 3.3 and the 3D model view of pyramidal horn antenna with and without PRS is shown in Fig. 3.14.

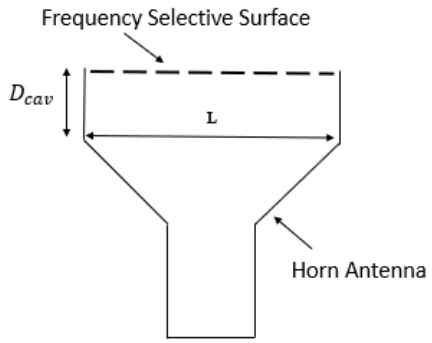

Fig. 3.12 Schematic View of Pyramidal Horn Antenna with Frequency Selective Surface (FSS)

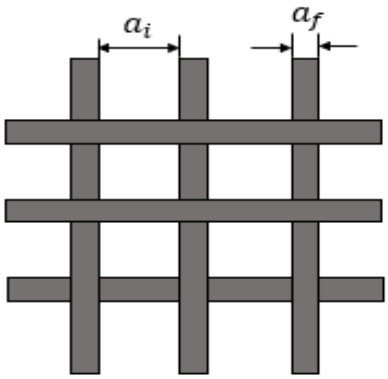

Fig. 3.13 Schematic View of Metallic Grid

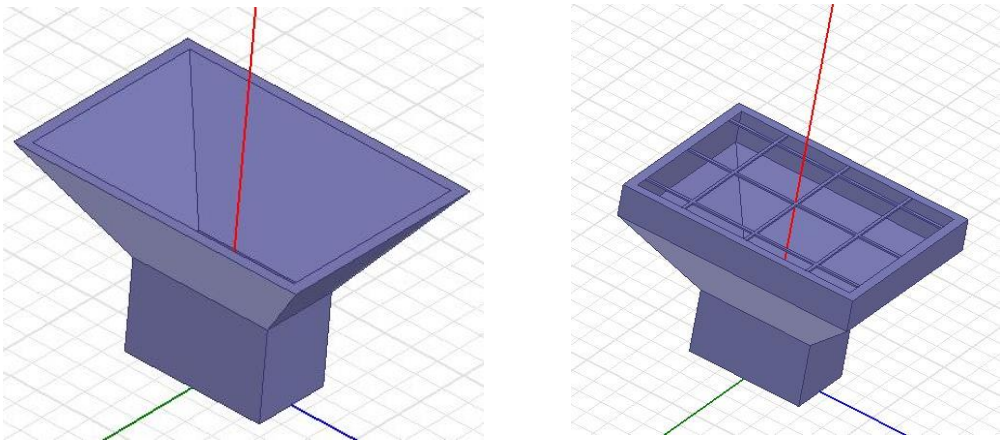

(a) (b)

Fig. 3.14 3D Model of a Pyramidal Horn Antenna (a) Without PRS and (b) With PRS designed in HFSS

Table 3.3 Dimensions of a pyramidal horn antenna with PRS

Parameters	**Values**
Design Frequency	2.64 GHz
Design Wavelength	113.45 mm
Rectangular Waveguide	86.36 mm × 43.18 mm
Antenna Aperture	198.6 mm × 145 mm
Grid Dimensions	a_f = *2.5 mm*, d_f = *1.5 mm*, a_i = *58 mm*
Cavity Height	D_{cav} = *28.3625 mm*

As discussed in chapter-2 about various types of partially reflecting surface and the dependency of their reflection characteristics on the dimensions of PRS structure, an exhaustive parametric analysis was carried on the designed pyramidal horn antenna with PRS.

1. Variation in Grid Dimensions (a_f, d_f and a_i)

The effect of varying grid dimension a_f on the gain of a pyramidal horn antenna is shown in Fig. 3.15. It is observed that there is an increase in gain by increasing the value of a_f, but at an expense of return loss which is not feasible. Hence a tradeoff is made for the mid-value dimension. After analyzing the results of parametric analysis over the entire frequency range, a suitable dimension for a_f was selected for designing a partially reflecting surface.

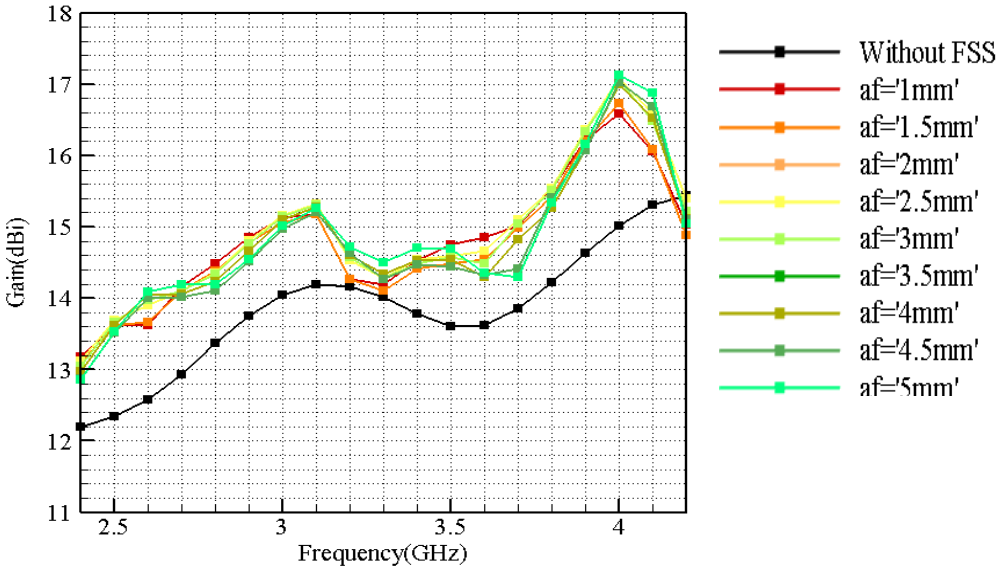

Fig. 3.15 Comparison of Gain for a Pyramidal Horn Antenna with PRS for different Values of a_f

Furthermore, the grid size and its inter-element spacing were varied and the results are shown in Fig. 3.16 and Fig. 3.17, respectively. It was observed that the variation in size of the grid does not contribute much to the gain of antenna whereas the variation in inter-element spacing affects the gain. From Fig. 3.17 it can be concluded that for a particular inter-element spacing an increment in gain is observed over the entire frequency range.

After comparing all the results of parametric analysis, optimum values for the metallic grid is chosen to design the partially reflecting surface for pyramidal horn antenna.

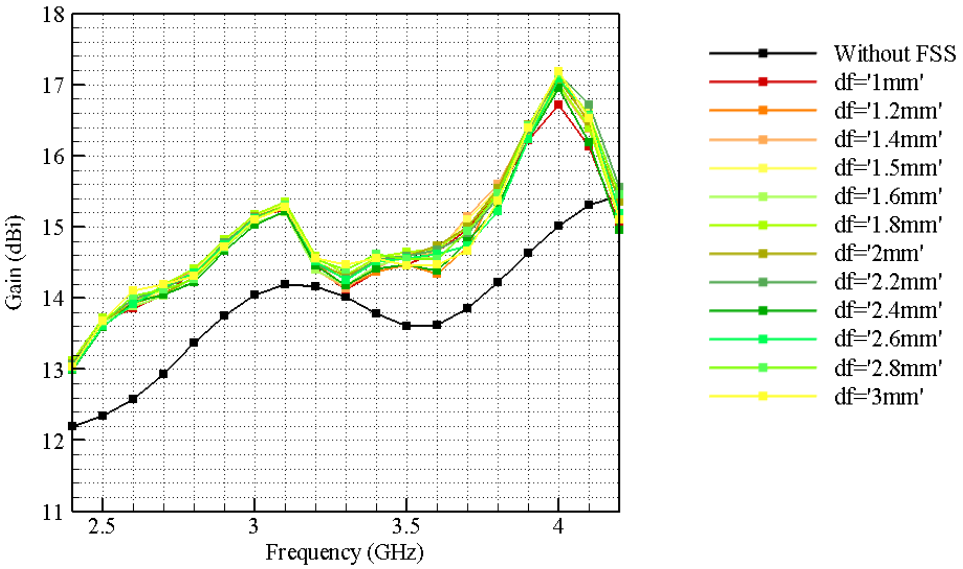

Fig. 3.16 Comparison of Gain for a Pyramidal Horn Antenna with PRS for different Values of d_f

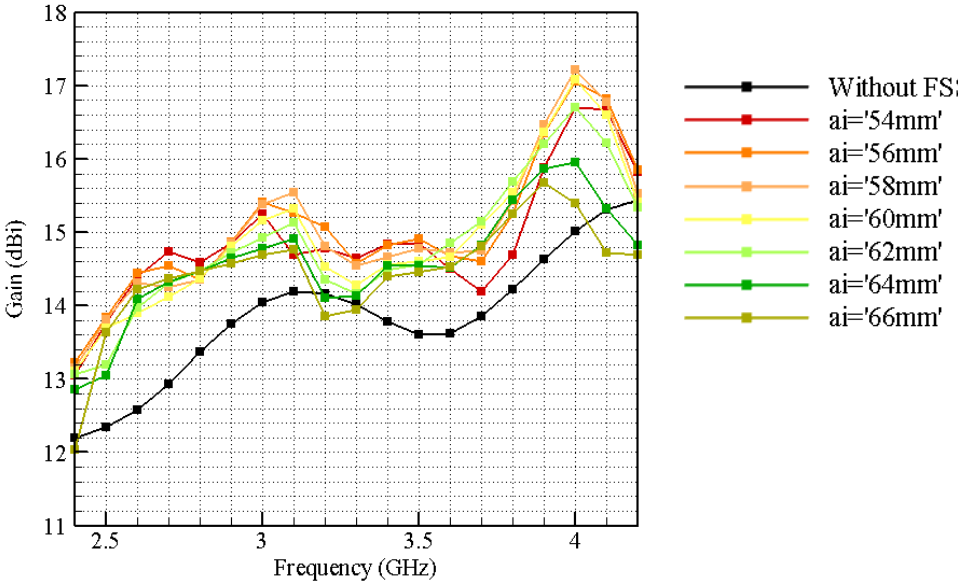

Fig. 3.17 Comparison of Gain for a Pyramidal Horn Antenna with PRS for different Values of a_i

2. Variation in Cavity Height (D_{cav})

The most crucial attribute while designing a Fabry-Perot antenna (FPA) is the distance between PRS and ground plane as the reflection of EM waves depends on it. It is referred to as cavity distance or height. The gain and bandwidth of FPAs depend on the cavity distance. According to the literature, partially reflecting surface is generally placed at a distance of half-wavelength from a ground plane or antenna aperture. Thus, to have the best suitable cavity distance, a parametric analysis was carried out for a pyramidal horn antenna by varying D_{cav} at an interval of $0 < \lambda < \frac{\lambda}{4}$ and $\frac{\lambda}{4} < \lambda < \frac{\lambda}{2}$.

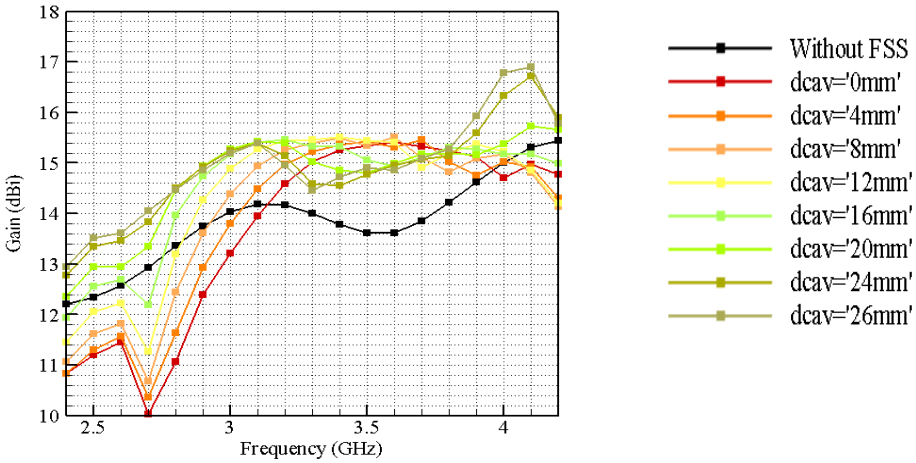

Fig. 3.18 Comparison of Gain of a Pyramidal Horn Antenna with PRS for D_{cav} between $0 < \lambda < \frac{\lambda}{4}$

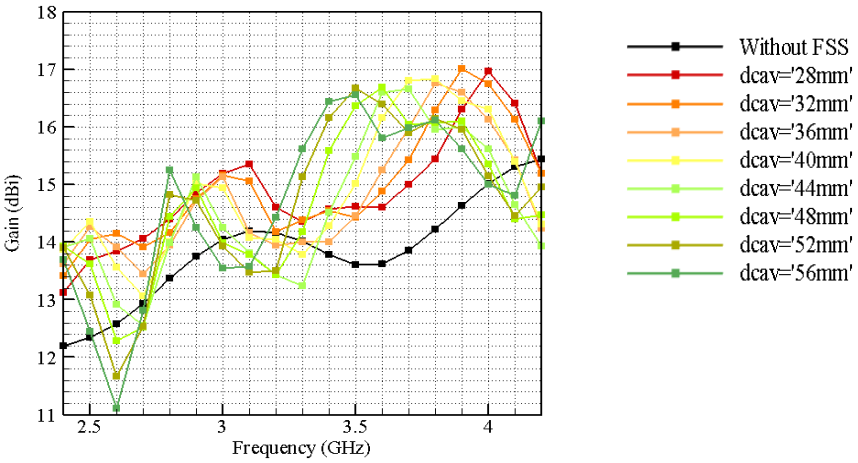

Fig. 3.19 Comparison of Gain of a Pyramidal Horn Antenna with PRS for D_{cav} between $\frac{\lambda}{4} < \lambda < \frac{\lambda}{2}$

From Fig. 3.18 and Fig. 3.19 it is observed that the variation in cavity distance significantly affects the gain of a pyramidal horn antenna. It can be observed that the region between $0 < \lambda < \frac{\lambda}{4}$, there is an improvement in the gain of an antenna over the entire range of frequency while for the region between $\frac{\lambda}{4} < \lambda < \frac{\lambda}{2}$, the gain of an antenna improves for some specific frequencies. After comparing it is concluded that the maximum gain is achieved at cavity distance of quarter wavelength (λ/4).

Based on the parametric analysis, the best combination of grid dimension and cavity distance were selected to design a pyramidal horn antenna with a partially reflecting surface. The simulated results for return loss and gain of the designed pyramidal horn antenna with and without PRS are shown in Fig. 3.20 and Fig. 3.21, respectively. From Fig. 3.20, it can be concluded that the addition of partially reflecting surface reduces the return loss at lower frequencies.

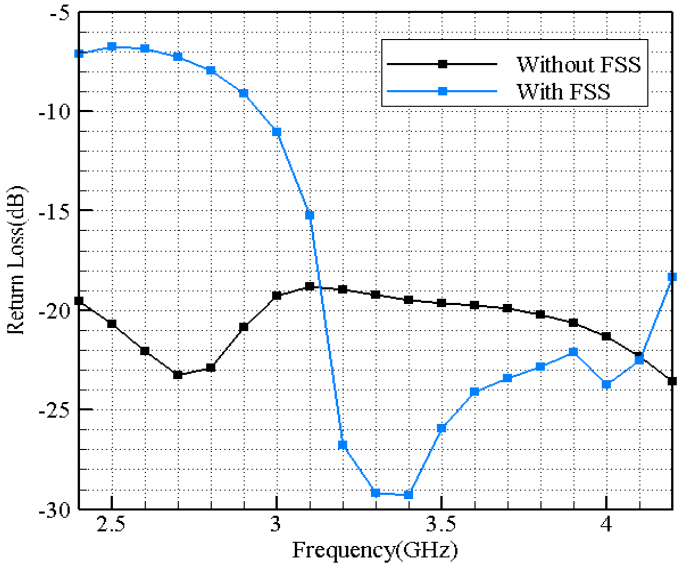

Fig. 3.20 Comparison of Return Loss of a Pyramidal Horn Antenna with and without PRS

Fig. 3.21 shows the gain plot of a pyramidal horn antenna with and without PRS, it is observed that there is an increment of 1 dB in gain performance over the entire range of frequency. The maximum gain increment of 2.21 dBi is obtained at a frequency of 4 GHz.

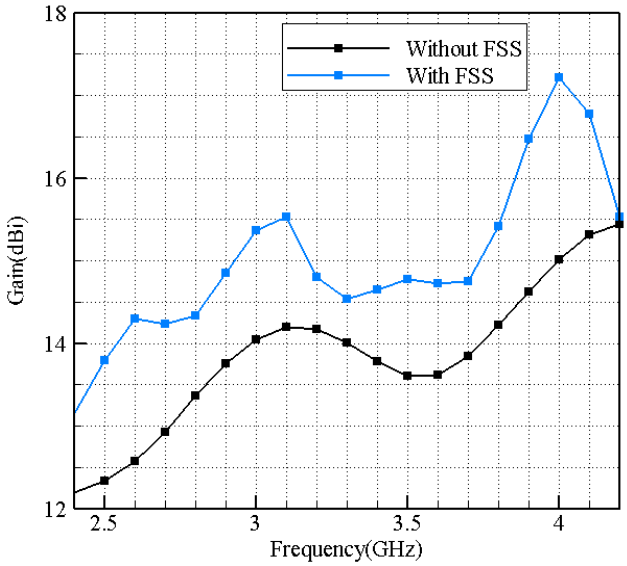

Fig. 3.21 Comparison of Gain of a Pyramidal Horn Antenna with and without PRS

Thus, we can conclude that the addition of partially reflecting surface to a pyramidal horn antenna at a distance of quarter wavelength from the aperture, contributes to an increment of gain with poor return loss performance at lower frequencies.

3.3 DESIGN OF A CONICAL HORN ANTENNA WITH AND WITHOUT PRS

A conical horn antenna is designed for frequency range 2.2-3.3 GHz. The main objective is to enhance the gain of the horn antenna by applying the concept of the Fabry-Perot cavity. The Fabry-Perot antenna is formed with three elements: a primary radiator (in this case we have chosen conical horn antenna), a partially reflecting surface (a frequency selective surface i.e. an inductive metal grid and a capacitive array of a metallic patch) placed at an appropriate distance from the antenna aperture or ground plane. According to the literature, there are various types of frequency selective surfaces with two major types as small metallic arrays of patches (capacitive) and metallic grid (inductive). Therefore, in this section, we have implemented both the types of FSS with a conical horn antenna for directivity and gain enhancement of the antenna.

The section is subdivided into two parts:

a. Conical horn antenna with metallic grid used as partially reflecting surface
b. Conical horn antenna with an array of metallic patch used as partially reflecting surface.

3.3.1 DESIGN-1 CONICAL HORN ANTENNA WITH METALLIC GRID AS PARTIALLY REFLECTING SURFACE

A conical horn antenna is designed for frequency range 2.2-3.3 GHz. The dimensions of the proposed design are given in Table 3.4 and the 3D model view of conical horn antenna with and without PRS is shown in Fig. 3.23.

Table 3.4 Dimensions of a Conical Horn Antenna with Metallic Grid as PRS

Parameters	Values
Design Frequency	2. 64 GHz
Design Wavelength	113.63 mm
Waveguide radius	54.26 mm
Antenna Aperture	159.54 mm
Grid Dimensions	a_f=1mm, d_f=1mm, a_i=60 mm
Cavity Height	D_{cav}= 26 mm

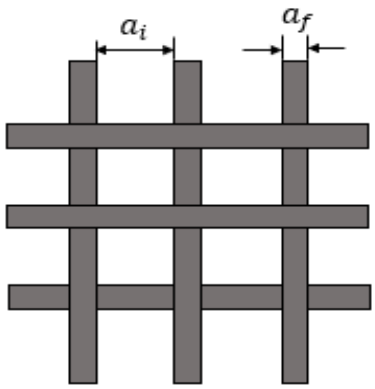

Fig. 3.22 Schematic View of Metallic Grid

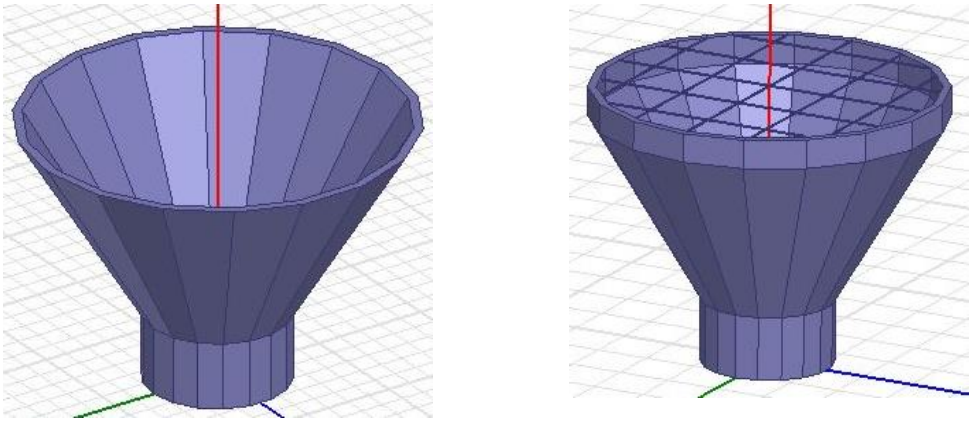

(a) (b)

Fig. 3.23 3D Model of a Conical Horn Antenna (a) Without PRS and (b) With PRS designed in HFSS

The amount of reflection from the metallic grid depends on its reflection coefficient and the distance between PRS and antenna aperture. The reflection coefficient of the grid can be varied by changing their dimension and interelement spacing between the grids. A full parametric analysis was carried out for designing an appropriate grid for a conical horn antenna.

1. Variation in Grid Dimensions (a_f and d_f)

The effect of varying grid dimension a_f is shown in Fig. 3.24. It is observed that there is significant variation in the performance of gain of an antenna by increasing the value of a_f, without much affecting the return loss. Hence, after analyzing the results of parametric analysis over the entire frequency range, a suitable dimension for a_f was selected for the design of partially reflecting surface.

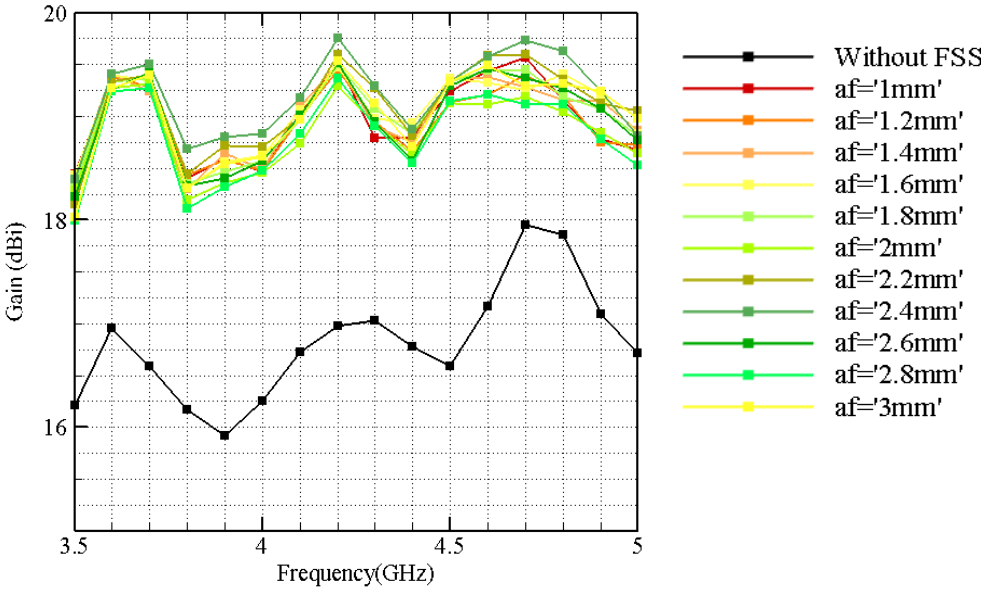

Fig. 3.24 Comparison of Gain for a Conical Horn Antenna with PRS for different Values of a_f

Furthermore, the grid size was varied and the result is shown in Fig. 3.25. It was observed that the variation in the size of the grid contributes in the increment of gain of an antenna. After comparing all the results of parametric analysis, optimum values for the metallic grid is chosen to design the partially reflecting surface for conical horn antenna.

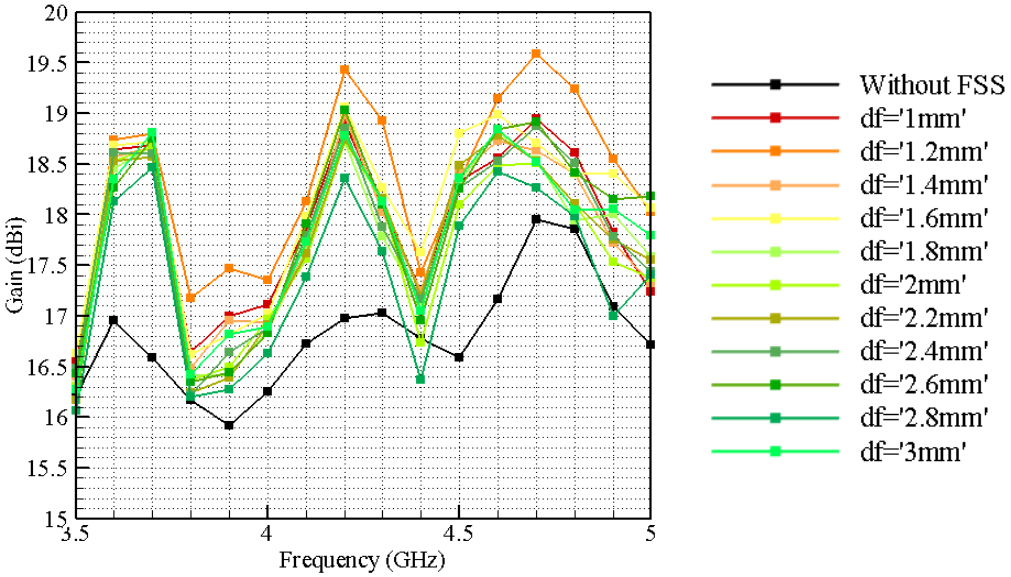

Fig. 3.25 Comparison of Gain for a Conical Horn Antenna with PRS for different Values of d_f

1. Variation in Cavity Height (D_{cav})

As the cavity distance is the most crucial attribute while designing a Fabry-Perot antenna (FPA), here we present a parametric analysis on gain of designed conical Fabry-Perot horn antenna by varying the cavity distance at an interval of $0 < \lambda < \frac{\lambda}{4}$ and $\frac{\lambda}{4} < \lambda < \frac{\lambda}{2}$.

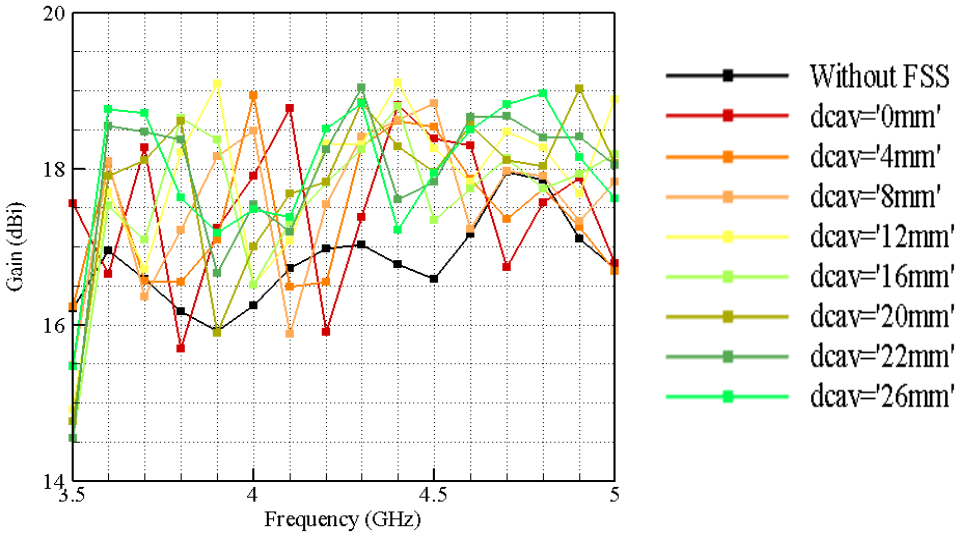

Fig. 3.26 Comparison of Gain of a Conical Horn Antenna with PRS for D_{cav} between $0 < \lambda < \frac{\lambda}{4}$

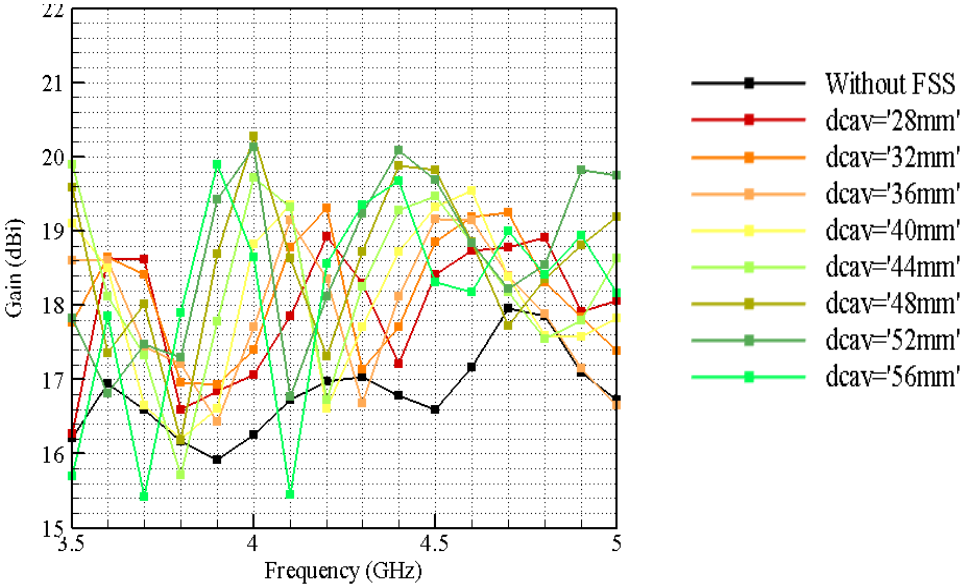

Fig. 3.27 Comparison of Gain of a Conical Horn Antenna with PRS for D_{cav} between $\frac{\lambda}{4} < \lambda < \frac{\lambda}{2}$

From Fig. 3.26 and Fig. 3.27 it is observed that the variation in cavity distance significantly affects the gain of a conical horn antenna. It can be observed that the region between $0 < \lambda < \frac{\lambda}{4}$, there is an improvement in a gain of an antenna over the entire range of frequency for quarter wavelength distance while for the region between $\frac{\lambda}{4} < \lambda < \frac{\lambda}{2}$, there is no improvement observed for the entire frequency range. After comparing it is concluded that the maximum gain is achieved at cavity distance at 26mm.

From the above parametric analysis, the best combination of grid dimension and cavity distance was selected to design the conical horn antenna with a partially reflecting surface. The simulated results for return loss and gain of the designed conical horn antenna with and without PRS are shown in Fig. 3.28 and Fig. 3.29 respectively.

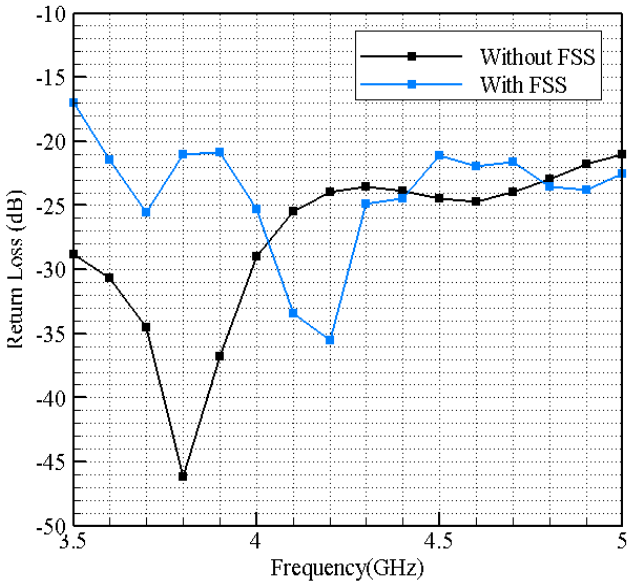

Fig. 3.28 Comparison of Return Loss of a Conical Horn Antenna with and without PRS

After comparing to the return loss of a conical horn with pyramidal horn antenna with PRS, it is observed that for the entire frequency range the return loss value < -15 dB which is acceptable for practical applications. Addition of partially reflecting surface to a conical horn antenna, there is an increment of more than 1 dB in a gain of an antenna over the entire frequency range. The maximum increment of 2.02 dBi is obtained at a frequency of 4.5 GHz.

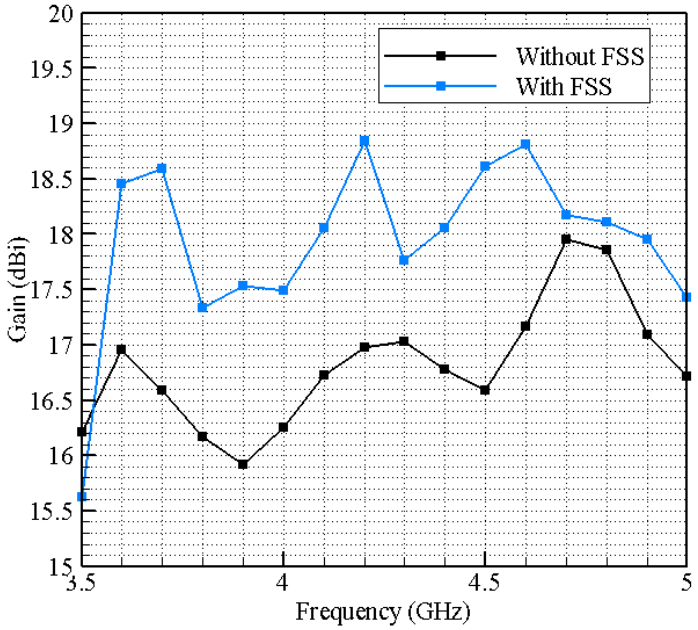

Fig. 3.29 Comparison of Gain of a Conical Horn Antenna with and without PRS

3.3.2 DESIGN-2 CONICAL HORN ANTENNA WITH ARRAY OF METALLIC PATCH AS PRS

A conical horn antenna is designed for frequency range 2.5-2.7 GHz. The design consists of an array of metallic patch used as partially reflecting surface and a metallic ground plane placed at a distance of half wavelength from the PRS. The conical FPA designed is different from the previous section in terms of the PRS used and the introduction of a ground plane. The dimension of the proposed design is given in Table 3.5 and the 3D model view of a conical horn antenna with and without PRS is shown in Fig. 3.31.

Table 3.5 Dimensions of a Conical Horn Antenna with an Array of Metallic Patches

Parameters	**Values**
Design Frequency	2.6 GHz
Design Wavelength	115.38 mm
Waveguide radius	25 mm
Antenna Aperture	110 mm
Patch Dimensions	a = 72 mm, d = 90 mm
Cavity Height	D_{cav}=60 mm

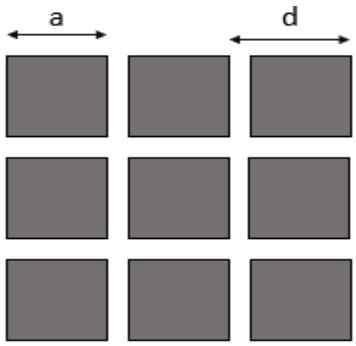

Fig. 3.30 Schematic View of Array of Metallic Patch

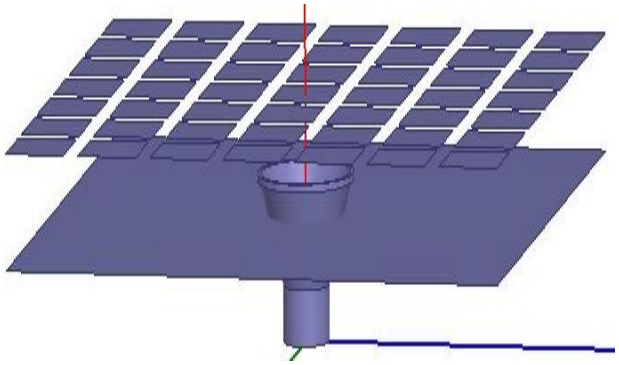

Fig. 3.31 3D Model View of a Conical Horn Antenna with PRS designed in HFSS

The reflection from the array of metallic patches depends on the number of patches and their configuration. Hence, parametric study was done by varying the number patch elements in the sheet of PRS.

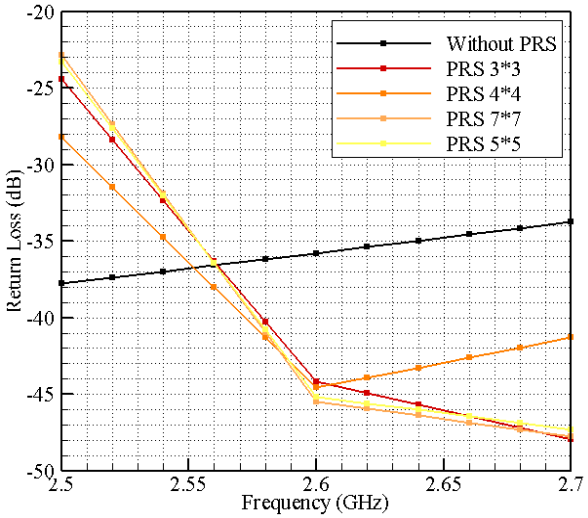

Fig. 3.32 Comparison of Return Loss of a Conical Horn Antenna with PRS for different Number of Patch Elements

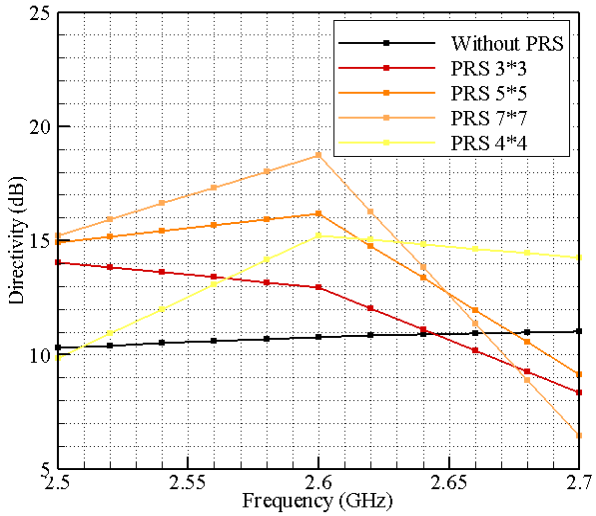

Fig. 3.33 Comparison of Gain of a Conical Horn Antenna with PRS for different Number of Patch Elements

Fig. 3.32 and Fig. 3.33 shows the simulated results of return loss and gain of a conical horn antenna with PRS for different configurations of the PRS layer, respectively. After comparing the results of parametric analysis, the maximum increment of gain is observed for 7×7 configuration of patch however, the gain increment is observed over the entire frequency range for 4×4 configuration of the patch. Thus, a conical horn antenna with 4×4 PRS configuration was simulated and results are shown in Fig. 3.34, Fig. 3.35, and Fig. 3.36 for return loss, directivity, and radiation patterns, respectively.

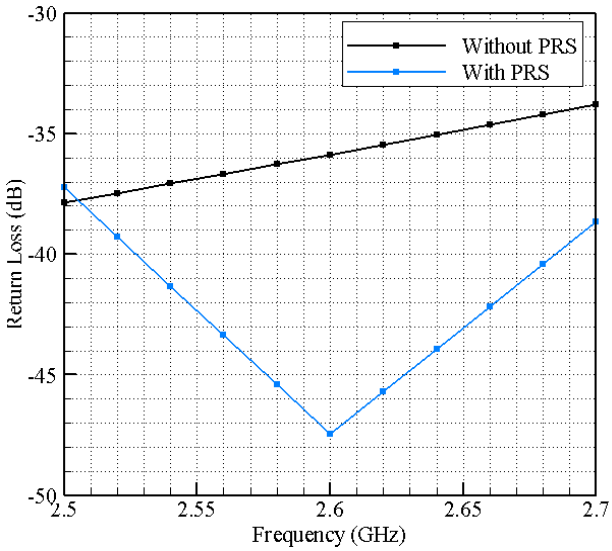

Fig. 3.34 Comparison of Return Loss of a Conical Horn Antenna with and without PRS (an Array of Metallic Patch)

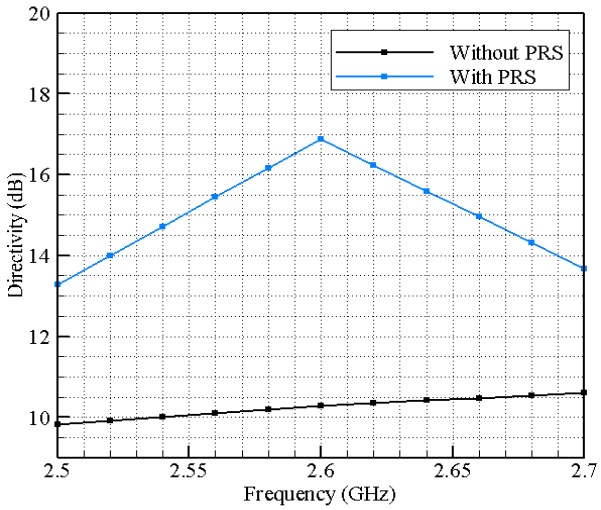

Fig. 3.35 Comparison of Directivity of a Conical Horn Antenna with and without PRS (an Array of Metallic Patch)

It can be observed that there is a significant increase of 6.58 dB in directivity at design frequency (2.6 GHz) compared to the result of a conical horn antenna without PRS. Also, there is a major improvement in the radiation pattern of horn antenna with PRS as shown in Fig. 3.36. With the addition of a PRS layer, the directivity pattern becomes narrower and there are very low sidelobe levels.

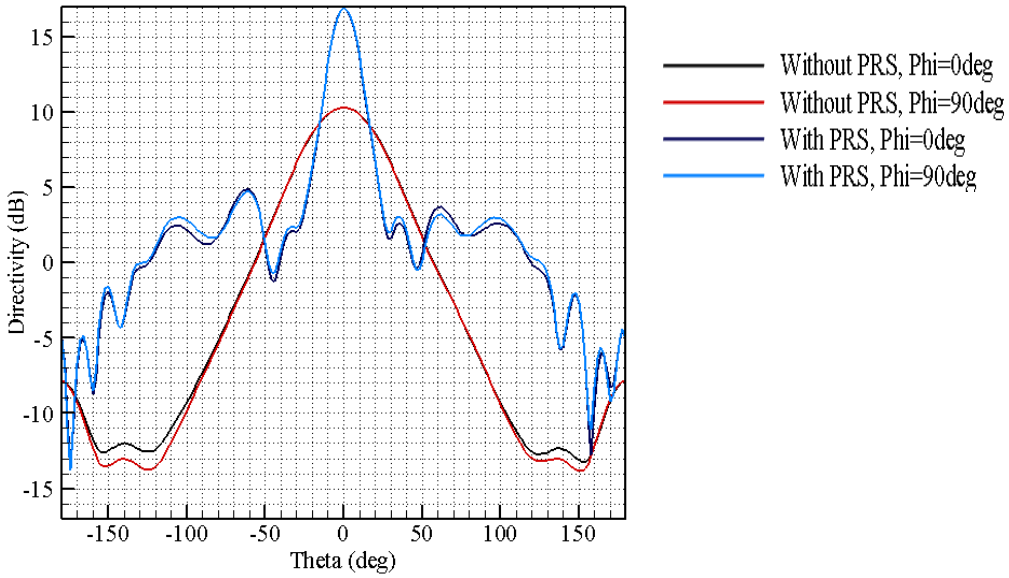

Fig. 3.36 Comparison of Radiation Pattern of a Conical Horn Antenna with and without PRS (an Array of Metallic Patch)

3.4 DESIGN OF CLUSTER OF CONICAL HORN ANTENNA WITH AND WITHOUT PRS

Horn antennas are widely used as feed for reflector antennas. The radiation pattern of a single antenna element generally provides a wide radiation pattern with low directivity and gain, but for long-distance communications, it is necessary to have high gain antennas. Thus, a cluster of horn antennas is formed to enhance the directivity performance. A cluster of horn antennas is a unique arrangement of the array of horn antenna generally used for satellite communications. As discussed in chapter-2 there are several configurations of forming a cluster of the horn antennas. This section discusses the design of a cluster of seven conical horn antennas with and without partially reflecting surfaces.

Some of the important features while designing an array of an identical element are,

a) the geometrical configuration of an overall array (cluster of horn antennas can be formed of 1-, 3- and 7-feed horn(s)),
b) the relative displacement between these individual elements,
c) the excitation amplitude and phase of an individual antenna, and
d) the individual radiation patterns.

The overall radiation pattern cluster of horn antennas is controlled by the above-mentioned features. The designed cluster of a conical horn antenna is shown in Fig. 3.37 and dimensions are given in Table 3.6.

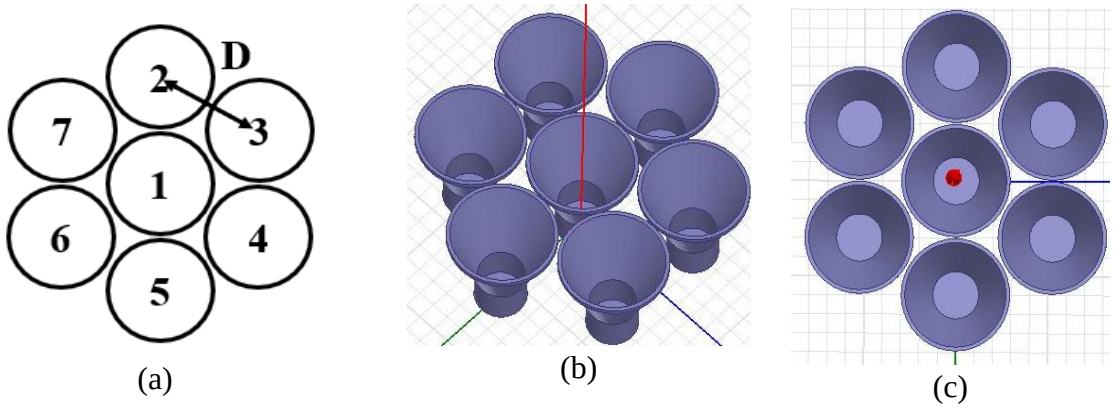

(a) (b) (c)

Fig. 3.37 Cluster of Seven Feed Configuration with (a) Schematic View, (b) and (c) 3D Model View designed in HFSS.

Table 3.6 Dimensions of a Conical Horn Antenna for Cluster

Parameters	**Values**
Design Frequency	2.6 GHz
Design Wavelength	115.38mm
Waveguide radius	25mm
Antenna Aperture	110mm
Center-to-center spacing	D = 120mm
Patch Dimensions	a = 72mm, d = 90mm
Cavity Height	D_{cav}=60mm

The cluster of conical horn antenna was simulated and results of return loss, directivity, and radiation pattern are shown in Fig. 3.38 and Fig. 3.39, respectively. From Fig. 3.38 it can be observed that the maximum directivity of 16.0 dB is obtained at 2.7 GHz and 15.88 dB at design frequency (2.6 GHz).

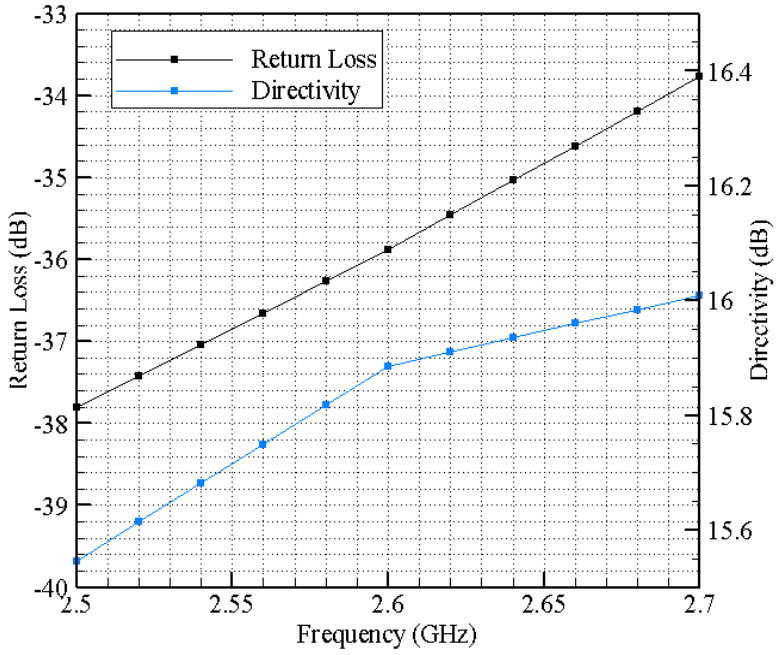

Fig. 3.38 Return Loss and Directivity of a Cluster of Conical Horn Antennas without PRS

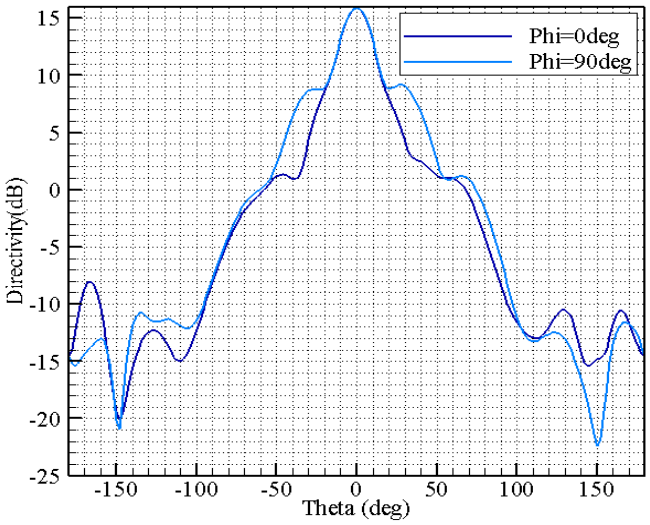

Fig. 3.39 Radiation Pattern of Cluster of Conical Horn Antennas

Addition of partially reflecting surface to a cluster of horn antennas is challenging task as the multiple reflection from PRS may disrupt the radiation pattern of the adjacent horn antenna and leads to poor directivity.

An array of 7×7 metallic patch is added to the cluster of conical horn antenna as a PRS layer at a distance of half-wavelength to form a Fabry-Perot cavity. However, this configuration resulted in a degradation of directivity of cluster of conical horn antennas. To overcome this limitation different configurations with variation in center-to-center spacing were designed to improve the directivity of a cluster of conical horn antenna. The design variations are depicted in Fig. 3.40 and the specifications are given in Table 3.7.

Table 3.7 Design details of Cluster of a Conical Horn Antenna with PRS

Design of Cluster	Center-to-Center Spacing	Number of Elements in an Array
Design-1	120 mm	7×7
Design-2	180 mm	7×7
Design-3	270 mm	7×7
Design-4	270 mm	8×8

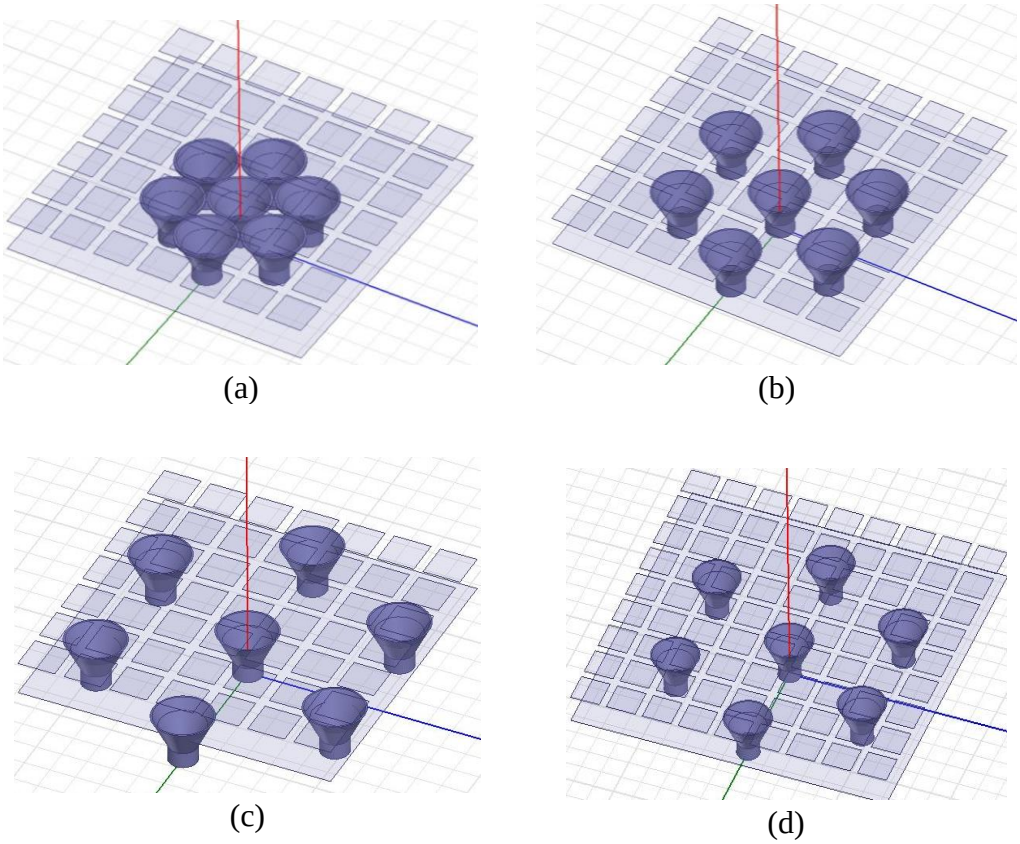

Fig. 3.40 Cluster of Conical Horn Antennas with PRS at (a) *D* =120 mm, (b) *D*=180 mm, (c) *D*=270 mm, and (d) *D*=270 mm, PRS 8×8

All the designs were simulated and the results of return loss and directivity are shown in Fig. 3.41 and Fig. 3.42, respectively.

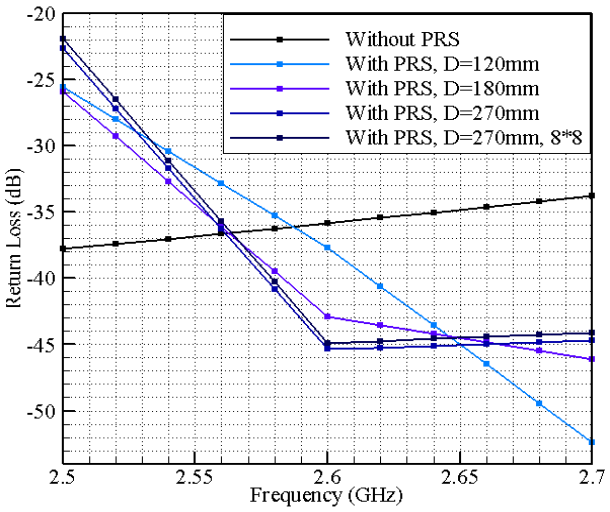

Fig. 3.41 Comparison of Return Loss of a Cluster of Horn Antennas for various Center-to-Center Spacing.

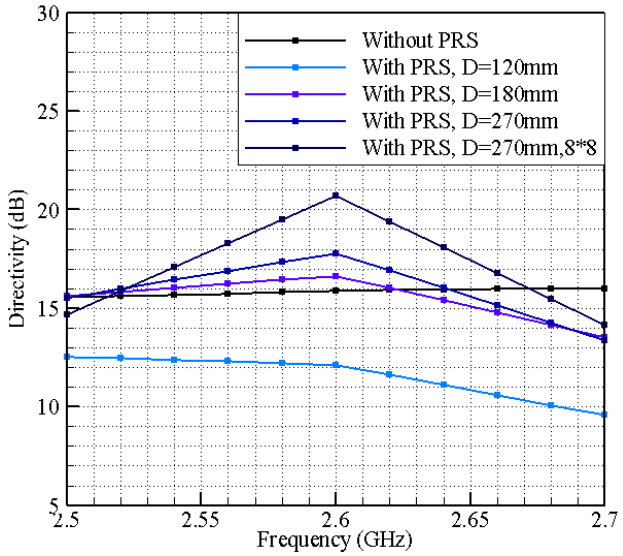

Fig. 3.42 Comparison of Directivity of a Cluster of Horn Antennas for various Center-to-Center Spacing.

After comparing the results, it can be concluded that with the increase in center-to-center spacing there was an improvement in the overall performance of directivity over an entire range of frequency. Table 3.8 shows the comparison between the directivity of all the four different configurations of cluster of conical horn antennas with PRS layer.

Table 3.8 Comparison of directivity for different configurations of cluster of conical horn antenna with and without PRS

Frequency (GHz)	Directivity (dB) without PRS	Directivity (dB) with PRS			
		Design-1	Design-2	Design-3	Design-4
2.5	15.54607	12.53919	15.6394	15.53547	14.6673
2.52	15.61385	12.4564	15.83867	15.9862	15.87244
2.54	15.68163	12.37362	16.03794	16.43693	17.07758
2.56	15.74941	12.29084	16.23721	16.88767	18.28272
2.58	15.81719	12.20806	16.43648	17.3384	19.48786
2.6	**15.88497**	**12.12527**	**16.63575**	**17.78913**	**20.693**
2.62	15.90976	11.6157	16.01811	16.90435	19.37998
2.64	15.93456	11.10612	15.40047	16.01958	18.06695

2.66	15.95935	10.59655	14.78284	15.1348	16.75393
2.68	15.98415	10.08697	14.1652	14.25002	15.4409
2.7	16.00895	9.577396	13.54756	13.36524	14.12788

From Table 3.8 it can concluded that there is an increment in directivity of cluster of conical horn antennas with partially reflecting surface for 270 mm center-to-center spacing and 8×8 array of metallic patch over the entire frequency range, with maximum increment of 4.81 dB at design frequency (2.6 GHz).

CHAPTER-4

CONCLUSION AND FUTURE SCOPE

In this chapter, all the results are summarized and important conclusions are listed. The future scope of work is also described.

4.1 Conclusions

The section is subdivided into four parts.

4.4.1 Conclusions on Circular Waveguide with Partially Reflecting Surface-

- Addition of a PRS layer at a specific distance improves the directivity of a circular waveguide.
- There are three different designs of a circular waveguide. Single-stage FP antenna is the simplest design in terms of fabrication, however, the presence of higher-order modes and side lobes in radiation pattern limits their use in practical applications.
- Addition of another layer of PRS helps in reducing the effects of higher order modes. While the addition corrugations reduce the sidelobe level and propagation of surface wave.
- The results for all the three configurations are summarized in Table 4.1. The maximum gain increment of 6.59 dBi is obtained for single stage Fabry-Perot antenna.

Table 4.1 Summary of maximum gain of circular waveguide with and without PRS

Sr. No.	Antenna	Maximum Gain (dBi)
1.	Circular Waveguide	8.73
2.	Single Stage FPA	15.32
3.	Stacked FPA	15.23
4.	Stacked FPA with corrugation	14.20

4.4.2 Conclusions on a Pyramidal Horn Antenna with Partially Reflecting Surface-

- Modeling and designing of an inductive metal grid as a partially reflecting surface must be precise in measurement, even a single and small change in the grid dimensions leads to disorder in return loss and directivity of an antenna.
- After parametric analysis, it is verified that the reflection characteristics of partially reflecting surface depends on the distance between the surface and antenna aperture, and the grid dimensions. Even a small variation in cavity distance alters the gain and return loss of a pyramidal horn antenna.
- The maximum increment of 2.21 dBi is obtained at 4 GHz with return loss less -7dB over the whole frequency range.

4.4.3 Conclusions on Conical Horn Antenna with Partially Reflecting Surface-

- There are two different configurations of partially reflecting surface being implemented for directivity and gain enhancement of conical horn antenna: metallic grid and an array of patch elements.
- Designing a frequency selective surface for a Fabry-Perot antenna is the most important attribute as the reflection characteristics of PRS layer depends on its reflection coefficient. And the reflection coefficient depends on the grid and patch dimensions.
- It was observed that the amount of reflection from a the designed PRS layer depends on:

✓ Distance between PRS layer and antenna aperture,

✓ Grid and patch dimension,

✓ Inter-element spacing (for metal grid the distance two grid and the distance between two array elements), and

✓ Number of patch element used in an array.

- With metallic grid as a partially reflecting surface, there is an increment of 2.02 dBi at 4.5 GHz in the gain of a conical horn antenna.
- With an array of a metallic patches as a partially reflecting surface, there is an increment of 6.58 dB at 2.6 GHz in a directivity of a conical horn antenna.

4.4.4 Conclusions on Cluster of Conical Horn Antenna with Partially Reflecting Surface-

- Designing of a cluster of horn antennas is a complex task as the overall radiation pattern of an antenna depends on the individual radiation pattern, the excitation amplitude; and phase of the individual element, the center-to-center spacing between the element, and the geometrical configuration of an array.
- The addition of partially reflecting surface to a cluster of horn antennas is a challenging task as the multiple reflections from PRS layer may disrupt the radiation pattern of the adjacent horn antenna and leads to poor directivity.
- Various configurations were designed and simulated; the results are summarized in Table 4.2.

Table 4.2 Summary of results of designed cluster of conical horn antennas with and without PRS layer.

Design of Cluster	**Directivity (dB) at 2.6GHz**		
Cluster without PRS	15.88		
Design of Cluster of Conical Horn Antennas with PRS			
Different Configurations	Center-to-Center Spacing	Number of Elements in an Array	Directivity (dB) at 2.6 GHz
Design-1	120 mm	7×7	12.12
Design-2	180 mm	7×7	16.63
Design-3	270 mm	7×7	17.78
Design-4	270 mm	8×8	20.69

- From Table 4.2 it can be concluded that the center-to-center spacing between the individual horn antenna supremely affects the directivity of cluster.
- There is an increment in directivity of cluster of conical horn antennas with partially reflecting surface for 270 mm center-to-center spacing between individual horn antenna and 8×8 array of metallic patch over the entire frequency range, with maximum increment of 4.81 dB at design frequency (2.6 GHz).

Thus, from all the above simulated designs of Fabry-Perot horn antenna it can be conclude that the addition of partially reflecting surface at a specific distance from antenna aperture enhances their directivity and gain performance.

4.2 Future Scope

- Implementation of Fabry-Perot cavity concept in horn antenna can be further be exploited by using different types of partially reflecting surfaces such as electromagnetic bandgap, dielectric, and metamaterial.
- The performance of a cluster of conical horn antenna with partially reflecting surfaces can be improved further by applying different configurations of PRS sheets.

REFERENCES

[1] G. V. Trentini, "Partially Reflecting Sheet Arrays", *IEEE Trans. Antennas Propag.*, vol. 4, pp. 666-671, October 1956.

[2] A. P. Feresidis and J. C. Vardaxoglou, "High Gain Planar Antenna using optimized Partially Reflective Surface," in *Proc. IEEE Microwaves, Antennas and Propagation*, vol. 148, pp. 345-350, Dec. 2001.

[3] R. Sauleau, Ph. Coquet, T. Matsui, and J. P. Daniel, "A New Concept of Focusing Antennas Using Plane-Parallel Fabry–Perot Cavities with Nonuniform Mirrors*", IEEE Trans. Antennas Propag.*, vol. 51, pp. 3171-3175 ,2003.

[4] S. A. Muhammad, R. Sauleau and H. Legay, "Small-Size Shielded Metallic Stacked Fabry–Perot Cavity Antennas with Large Bandwidth for Space Applications", *IEEE Trans. Antennas Propag.*, vol. 60, pp. 792-802, February 2012.

[5] Q. Chen, X. Chen and K. Xu, "3-D Printed Fabry–Perot Resonator Antenna with Paraboloid-Shape Superstrate for Wide Gain Bandwidth", *Journal of Applied Science*, vol. 7, pp. 1-11, November 2017.

[6] O. Ronciere, B. A. Arcos, R. Sauleau, K. Mahdjoubi, and H. Legay, "Radiation Performance of Purely Metallic Waveguide-Fed Compact Fabry-Perot Antennas for Space Applications," *Microwave and Optical Technology Letters*, vol. 49, pp. 2216-2221, June 2007.

[7] Ph. Coquet, R. Sauleau, U. Theuroudc, J.P. Daniel and T. Matsui, "57GHz Gaussian beam antenna for wireless broadband communications", *Electron. Lett*., vol. 36, no. 7, pp. 594-596, 2000.

[8] N. Guerin, S. Enoch, G. Tayeb, P. Sabouroux, P. Vincent and H. Legay, “A metallic Fabry-Perot directive antenna”, *IEEE Trans. Antennas Propag.*, vol. 54, pp. 220-224, January 2006.

[9] Y. Ge, K. P. Esselle and T. S. Bird, “The Use of Simple Thin Partially Reflective Surfaces with Positive Reflection Phase Gradients to Design Wideband, Low-Profile EBG Resonator Antennas”, *IEEE Trans. on Antennas Propag.*, vol. 60, pp. 743-750, February 2012.

[10] R. Weily, L. Horvath, K. P. Esselle, B. C. Sanders, and T. S. Bird, “A Planar Resonator Antenna Based on a Woodpile EBG Material”, *IEEE Trans. on Antennas Propag.*, vol. 53, pp. 216-223, January 2005.

[11] C. Cheype, C. Serier, M. Thevenot, T. Monediere, A. Reineix and B. Jecko, "An electromagnetic bandgap resonator antenna”, *IEEE Trans. on Antennas Propag.*, vol. 50, pp. 1285-1290, September 2002.

[12] Y. Ge, K. P. Esselle and T. S. Bird, “Designing a partially reflective surface with increasing reflection phase for wide-band EBG resonator antennas”, *IEEE Antennas Propag. Society Int. Symp.*, Charleston, SC, pp. 1-4, 2009.

[13] C. A. Balanis, *Antenna Theory: Analysis and Design*., John Wiley & Sons, Inc., Hoboken: New Jersey, 2005.

[14] D. Jackson and N. Alexopoulos, “Gain enhancement methods for printed circuit antennas”, *IEEE Trans. on Antennas Propag.*, vol. 33, pp. 976-987, September 1985.

[15] H. Yang and N. Alexopoulos, “Gain enhancement methods for printed circuit antennas through multiple superstrates”, *IEEE Trans. on Antennas Propag.*, vol. 35, pp. 860-863, July 1987.

[16] D. R. Jackson and A. A. Oliner, “A leaky-wave analysis of the high-gain printed antenna configuration”, *IEEE Trans. on Antennas Propag.*, vol. 36, pp. 905-910, July 1988.

[17] J. R. James, S. J. A. Kinany, P. D. Peel and G. Andrasic, “Leaky-wave multiple dichroic beamformers”, *Electron. Lett.*, vol. 25, no. 18, pp. 1209-1211, August 1989.

[18] D. R. Jackson, A. A. Oliner and A. Ip, “Leaky-wave propagation and radiation for a narrow-beam multiple-layer dielectric structure”, *IEEE Trans. on Antennas Propag.*, vol. 41, pp. 344-348, March 1993.

[19] R. Sauleau, G. Le. Ray, and Ph. Coquet, “Parametric Study and Synthesis of 60GHz Fabry-Perot Resonators”, *Microwave and Optical Technology Letters*, vol. 34, no. 4, pp. 247-252, August 2002.

[20] R. Sauleau, Ph. Coquet, D. Thouroude and J.-P Daniel, “Beam focusing using 60 GHz Fabry-Perot resonators with uniform and non-uniform metal grids”, *Electron. Lett.*, vol. 39, no. 4, pp. 341-342, February 2003.

[21] S. A. Muhammad, R. Sauleau and H. Legay, “Purely Metallic Waveguide-Fed Fabry–Perot Cavity Antenna with a Polarizing Frequency Selective Surface for Compact Solutions in Circular Polarization”, *IEEE Antennas and Wireless Propag. Lett.*, vol. 11, pp. 881-884, July 2012.

[22] Y. Ge, K. P. Esselle and T. S. Bird, “Designing a partially reflective surface with increasing reflection phase for wide-band EBG resonator antennas”, *IEEE Antennas Propag. Society Int. Symp.*, Charleston, SC, pp. 1-4, 2009.

[23] H. F. Shaban, H. A. Elmikaty, and A. A. Shaalan, “Study the effects of EBG substrate on two patches microstrip antenna”, *Progress In Electromagnetics Research (PIER B)*, vol. 10, pp. 55–74, January 2008.

[24] K. Konstantinidis, A. P. Feresidis, and P. S. Hall, “Multilayer Partially Reflective Surfaces for Broadband Fabry-Perot Cavity Antennas”, *IEEE Trans. on Antennas Propag.*, vol. 62, pp. 3474-3481, 2014.

[25] A. P. Feresidis and J. C. Vardaxoglou, "A broadband high-gain resonant cavity antenna with single feed", *1st European Conf. on Antennas Propag.*, Nice France, pp. 1-5, 2006.

[26] F. Qin, Steven Gao, Gao Wei, Qi Luo, Chunxu Mao, Chao Gu and Jiadong Xu, "Wideband Circularly Polarized Fabry-Perot Antenna", *IEEE Antennas and Propagation Magazine*, vol. 57, no. 5, pp. 127-135, October 2015.

[27] A. Lalbakhsh, M. U. Afzal, K. P. Esselle, and S. L. Smith, "Wideband Near-Field Correction of a Fabry–Perot Resonator Antenna," *IEEE Trans. on Antennas Propag.*, vol. 67, pp. 1975-1980, March 2019.

[28] W. Cao, X. Lv, Q. Wang, Y. Zhao and X. Yang, "Wideband Circularly Polarized Fabry–Perot Resonator Antenna in Ku-Band", *IEEE Antennas and Wireless Propag. Lett.*, vol. 18, no. 4, pp. 586-590, April 2019.

[29] S. A. Muhammad, R. Sauleau and H. Legay, "Low profile metallic self-polarizing Fabry-Perot cavity antenna", *7th European Conference on Antennas and Propagation (EuCAP)*, Gothenburg, pp. 3762-3765, 2013.

[30] H. Moghadas, M. Daneshmand and P. Mousavi, "Compact beam-reconfigurable feed for large aperture antennas", *IET Microwaves, Antennas and Propag.*, vol. 10, pp. 1159-1166, 2016.

[31] A. R. Weily, T. S. Bird and Y. J. Guo, "A Reconfigurable High-Gain Partially Reflecting Surface Antenna", *IEEE Trans. on Antennas Propag.*, vol. 56, pp. 3382-3390, November 2008.

[32] Q. Guo and H. Wong, "Wideband and High-Gain Fabry–Perot Cavity Antenna with Switched Beams for Millimeter-Wave Applications", *IEEE Trans. on Antennas Propag.*, vol. 67, pp. 4339-4347, July 2019.

[33] H. Attia, M. L. Abdelghani and T. A. Denidni, “Wideband and High-Gain Millimeter-Wave Antenna Based on FSS Fabry–Perot Cavity”, *IEEE Trans. on Antennas Propag.*, vol. 65, pp. 5589-5594, October 2017.

[34] K. Yao, S. Lan and L. Xu, “A high gain Fabry-Perot cavity antenna with a double-layered partially reflecting frequency selective surface structure”, *Int. Symp. on Antennas and Propagation (ISAP)*, Phuket, 2017.

[35] R. Sauleau, D. Thouroude, Ph. Coquet, and J. P. Daniel, “Theoretical reflection coefficient of Metal Grid reflectors at a dielectric interface”, *International Journal of Infrared and Millimeter Waves*, vol. 20, no. 2, 1999.

[36] R. Sauleau, P. Coquet, D. Thouroude, J. -. Daniel and T. Matsui, “Radiation characteristics and performance of millimeter-wave horn-fed Gaussian beam antennas”, *IEEE Trans. on Antennas Propag.*, vol. 51, pp. 378-387, March 2003.

[37] Q. Guo and H. Wong, “A Millimeter-Wave Fabry–Pérot Cavity Antenna Using Fresnel Zone Plate Integrated PRS”, *IEEE Trans. on Antennas Propag.*, vol. 68, pp. 564-568, January 2020.

[38] Lee, R. Sainati, and R. R. Franklin, “Frequency Selective Surface Effects on a Coplanar Waveguide Feedline in Fabry–Perot Cavity Antenna Systems”, *IEEE Antennas and Wireless Propag. Lett.*, vol. 17, no. 5, pp, 768-772, May 2018.

[39] R. S. Anwar, L. Mao, and H. Ning, “Frequency Selective Surfaces: A Review”, *Journal of Applied Science*, vol. 8, no. 9, pp. 1-47, 2018.

[40] T. K. WU, N. Grumman, and R Beach, “Frequency Selective Surfaces”, Encyclopedia of RF and Microwave Engineering, 2005.

[41] N. Wang, Q. Liu, C. Wu, L. Talbi, Q. Zeng and J. Xu, "Wideband Fabry-Perot Resonator Antenna With Two Complementary FSS Layers", *IEEE Trans. on Antennas Propag.*, vol. 62, pp. 2463-2471, May 2014.

[42] I. S. Syed, Y. Ranga, L. Matekovits, K. P. Esselle and S. Hay, "A Single-Layer Frequency-Selective Surface for Ultrawideband Electromagnetic Shielding", *IEEE Trans. on Electromagnetic Compatibility*, vol. 56, pp. 1404-1411, December 2014.

[43] S. A. Hosseini, F. De Flaviis and F. Capolino, "A highly-efficient single-feed planar Fabry-Pérot cavity antenna for 60 GHz technology", in *Proc. IEEE ISAP*, Chicago, IL, 2012.

[44] Z. Liu, "Broadband Fabry-Perot cavity leaky wave antenna with parabolic-shape reflector", *IEEE Asia-Pacific Conf. on Antennas Propag. (APCAP)*, Kaohsiung, 2016.

[45] A. P. Feresidis, K. Konstantinidis, and P. Gardner, "Fabry-Perot Cavity Antennas" in Aperture Antennas for Millimeter and Sub-Millimeter Wave Applications, France: Springer Publication, ch. 7, pp. 221-241.

[46] Z. Liu, "Fabry-Perot Resonator Antenna", in *Journal Infrared millimeter and terahertz waves*, springer publication, 2010.

[47] P. O. Iversen, L. J. Ricardi and W. P. Faust, "A comparison among 1-, 3-, and 7-horn feeds for a 37-beam MBA", *IEEE Trans. on Antennas Propag.*, vol. 42, pp. 1-8, January 1994.

[48] S. K. Rao, "Design and analysis of multiple-beam reflector antennas", *IEEE Antennas and Propag. Magazine*, vol. 41, pp. 53-59, August 1999.

[49] S. Rao, L. Shafai, and S. K. Sharma, "Handbook of Reflector Antennas and Feed Systems Volume III Applications of Reflectors".

[50] An Introduction to HFSS: Fundamental Principles, Concepts, and Use, Ansoft, LLC., Pittsburgh, Pennsylvania, USA, 2009.

PUBLICATION BASED ON THE THESIS

Submitted paper in

Conference Name-2020 IEEE International Symposium on Antennas and Propagation and North American Radio Science Meeting.

Title- Fabry-Perot Horn Antenna with Improved Gain.
Authors- Honey Dhandhukia, Dhaval Pujara.